ADDIS ABABA UNIVERSITY

SCHOOL OF GRADUATE STUDIES

GEOPHYSICAL INVESTIGATION FOR GROUND WATERPOTENTIAL ASSESSMENT AND MAPPING STRUCTURES AT ALIDEGE PLAIN, SOUTH AFAR, ETHIOPIA

BY

TEWODROS MULUGET CHICHAYBELU

A THESIS SUBMITTED TO THE SCHOOL OF GRADUATE STUDIES OF ADDIS ABABA UNIVERSITY IN PARTIAL FULFILMENT OF THE REQUIREMENTS FOR THE DEGREE OF MASTER OF SCIENCE IN EXPLORATION GEOPHYSICS

JUNE, 2011

Addis Ababa University

School of Graduate Studies

Department of Earth Sciences

GEOPHYSICAL INVESTIGATION FOR GROUND WATERPOTENTIAL ASSESSMENT AND MAPPING STRUCTURES AT ALIDEGE PLAIN, SOUTH AFAR, ETHIOPIA

By
Tewodros Mulugeta Chichaybelu

Approved by board of examiners:

Dr. Tigistu Haile Signature _____

Chairman, Department of Earth sciences

Dr.Tigistu Haile Signature_____

Advisor

Dr._____ Signature _____

Internal Examiner

Dr. _____ Signature _____

External Examiner

ACKNOWLEDGEMENT

First of all, I would like to thank the almighty God for everything He does in my life. I have nothing to say to my advisor Dr.Tigistu Haile for his crucial comments and sound suggestions that he gave me in order to accomplish this thesis successfully. During the time that I engaged in this work, he acted like not only my advisor but also like my father and colleague. I thank you for everything that you did for me.

I would like to say thank for Dr.Tilahun Mamo who helped me to arrange class schedule and give supportive suggestion and advice.

I am also thankful to the water works design and supervision enterprise office where I got the resistivity data, lithologic logs and geological reports of the study area and Department of Earth Sciences.

My thanks go also to my friends Tagel Assefa, Mulugeta chanie and Yahya Ali for their support to use different softwares to process the geophysical data.

Last but not least, I thank you to all my family and friends for their support and encouragement during the period of this work.

ABSTRACT

Vertical Electrical Sounding data collected over the Alidege Plain, located in the Zone 2, of the Afar Regional State has been used in this work. The plain is an extensive flat northeast-southwest running plain in the middle Awash valley with an average width of 26-30Kms and length of more than 70kms. The objective of the VES survey was to make an assessment of the groundwater potential of the plain, with a view to developing the plain both for agricultural and pastoral uses.

A total of 90 VES, collected at different field campaigns by the Water Works Design and Supervision Enterprises, has been used. The VES are well distributed over the plain and also a good number of the VES are aligned to enable one to construct a number of sections to depict the subsurface geology of the area. All the VES were individually first interpreted, and to aid in the interpretation of the data, the data were further presented in the form of apparent resistivity pseudodepth sections, sliced-stacked pseudodepth depth sections and true resistivity 2D geoelectric sections. A number of available boreholes distributed over the area were also used to calibrate the VES interpretation.

From the combination of these interpretations, it is found that the Alidege plain has adequate groundwater potential with the thick layers of moderately to highly fractured basalts and ignimbrite bearing the good portion of the groundwater resource. A number of structures have also been mapped at varying depths that could control the movement of groundwater and also aid in the location of productive boreholes. From the sliced-stacked pseudodepth sections, it has also been possible to show the direction of regional groundwater movement in the subsurface to be from northeast direction towards southwest direction.

TABLE OF CONTENETS PAGE

LIST OF FIGURES PAGE

LIST OF TABLES PAGE

ACRONYMS

BH	Borehole
EC	Electrical Conductivity
HD	Hand-dug well
Hrs	Hours
Km	Distance-Kilo Meter
Lat	Latitude
Long	Longitude
PET	Potential Vapor-transpiration
PVC	Poly Vinyl chloride
S	Spring
SWL	Static Water Level
SDR	Standard dimension ratio
TDS	Total Dissolved Solids
TOR	Terms of Reference
USSS	United States Salinity laboratory
UTM	Universal Transverse Meridian
UTME	Universal Transverse Mercator Easting
UTMN	Universal Transverse Mercator Northing
VES	Vertical Electrical Sounding
WFB	Wonji Fault Belt
WWDSE	Water Works Design & Supervision Enterprises

CHAPTER ONE
INTRODUCTION

1.1 General

Water is one of the basic needs to sustain life. Living things such as humans, animals and plants are dependent on water. Our bodies need to ingest water every day to continue functioning. Communities and individuals can exist with out many things like shelter, even with out food for a period, but they can not be deprived of water and survive for more than a few days. Because of the intimate relationship between water and life, it plays a vital role in the development of community since reliable supply of water is an essential perquisite for the establishment of a permanent community.

Access to clean water is a human right and a basic requirement for economic development. The safest kind of water supply is the use of groundwater. Since groundwater normally has a natural protection against pollution by the covering layers, only minor water treatment is required.

The largest amount of water on Earth (97.2 %) is contained in the oceans and seas as a saline or salty water but only small amount of it (2.8 %) exist as fresh water on land. This fresh water found on land is distributed as ice caps and glaciers (76.43 %), groundwater and soil moisture (21.96 %), fresh-water lakes (0.32%), saline-lakes (0.29 %) and very small amount of it as streams channels (0.004 %) (Fetter, 2001). The amount of fresh water which is available for domestic, industrial and agriculture purposes is very limited as compared to the total volume of water on the planet earth. Due to the above reasons, the search for ground water is vital as an immediate and sustainable solution to alleviate the scarcity of water for drinking and other domestic uses inmost part of the world as well as in Ethiopia.

In many developing countries there is not only a heavy reliance on groundwater as a primary drinking supply, either collected from shallow depth dug wells or from springs, but also as a supply of water for both agriculture and industrial use. The reliance on groundwater both in the developed and developing countries is such that it is necessary to ensure that there are significant

quantities of water and that the water is of a high quality. In addition to being clean through the natural process of filtration while passing through geological formations and thus being suitable for domestic consumption, ground water provides with replenishable and pollution free natural resource.

The use of geophysics for both groundwater resource mapping and for water quality evaluations has increased dramatically over the last 10 years in large part due to the rapid advances in microprocessors and associated numerical modeling solutions that facilitated the rapid acquisition and processing of data and their presentation in useful form (Shakeel, 2006). The use of geophysics for groundwater studies has also been stimulated in part by a desire to reduce the risk of drilling dry holes and also a desire to offset the costs associated with poor groundwater production. Today, the geophysicist also provides useful parameters for hydrogeological modeling of both new groundwater supplies and for the evaluation of existing groundwater contamination.

In this respect, the major objectives of this study are to identify potential areas for extraction of groundwater resources within the Alidege plain of the Afar Region and minimize the risk of sinking boreholes at inappropriate areas through the use of geophysical techniques. Specifically, the technique employed involves Vertical Electrical Sounding surveys over the wider areas of the plain so as to get a general assessment of its groundwater resource.

1.2 Description of the Study Area

1.2.1 Location and accessibility

The Alidege plain is located within the East African Rift System- a part of the complete tectonic feature of down faulted troughs extending from Mozambique in the south, northwards through East Africa, the horn of Africa, the Red sea and into Israel and Jordan extending for about 5000 kms- passing over Ethiopia and at the southern part of the Afar Rift just before the Rift narrows to the Main Ethiopian Rift. It lies in the low lying and northern part of the Main Ethiopian Rift, in Zone-2 of the Afar National Regional State and encompasses the areas surrounding Awash

Arba town. While most part of the Allaidege surface water catchments area is located within the Ethiopian Rift, its eastern extreme part occurs within the eastern Ethiopian plateau.

Specifically, Alidege plain is located in the middle Awash valley about 240 km northeast of Addis Ababa along the main asphalt road from 'Addis Ababa' towards 'Semera' via Gewane. The area is enclosed with approximate coordinates between 625000 UTME-673000UTME and 1008000UTMN-1067000 UTMN. The plain is an elongated flat lying ground oriented nearly north-south direction with a total length of more than 70 km and an average width of 25 km. The plain is bordered by Asebot Mountain in the east and by Awash River in the west (Figure 1.1).

Its origin is considered to be a tectonic development forming an intermountain trough. The main axis of the trough runs in a N-S direction. The frame of the trough is mainly composed of Tertiary volcanic rocks. That part of the plain near by the Awash River is dominantly composed of poorly compacted sedimentary basin fill deposits. The surficial topography of the area shows that surface water catchments drain in to the Awash River both from the East and West.

En echelon arrays of normal faults are the main causes of the surface topography of the Alidege plain. The last phase of these faulting, the Wonji Fault Belt, has created the two major plain of the area, the Alidege valley and the Awash valley. These valleys are separated by a horst of lava-gravel sequence. The western and eastern frames of the valley are composed of Tertiary basalts and it forms a high altitude difference (WWDSE, 2008 and the references there in). The eastern margin of the Allaidege valley is marked by the rhyolitic volcanic centers (Asebot, Afdem). Awash Arba, Mieso and other perennial streams rising from this eastern part drain westwards to feed the Awash River. Streams rising in the western part also flow east to feed the northwards flowing Awash River. The main Awash River course follows the steep northerly and northeasterly structures of the underlying volcanic rocks, the Wonji Fault Belt.

1.2.2 Climate and Vegetation

The climate of the Awash basin comes under the influence of the Inter Tropical Convergence Zone (ITCZ). This zone of low pressure marks the convergence of dry tropical easterlies and the moist equatorial easterlies. The seasonal rainfall distribution within the study area results from

the annual migration of the ITCZ. The ITCZ starts its advance across the study area from south in March bringing small spring rains. From June to September the ITCZ moves rapidly from north part of the country to the study area bringing heavy or summer rain. Along with the ITCZ the orography has significant effect for the formation of rain in the study area.

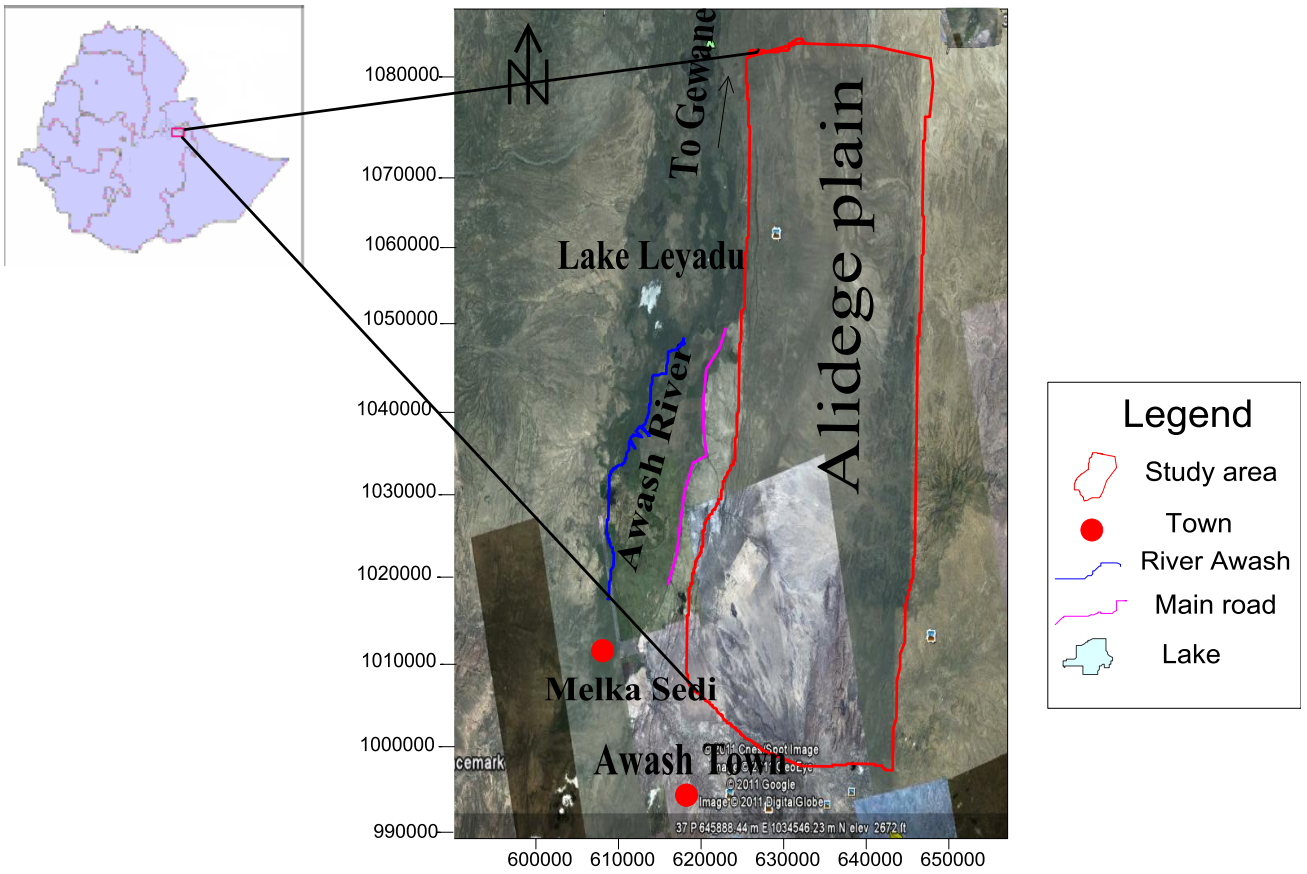

Figure 1.1 Location map of the study area

Comparison of monthly rainfall at various stations that differ in the amount of rainfall they receive can be done using the rainfall coefficient concept, as outlined in the FAO study (FAO, 1965). The rainfall coefficient is defined as the mean monthly rainfall divided by 1/12 of the annual mean rainfall. A “rainy” month was defined as one with a rainfall coefficient exceeding 0.6. The rainfall coefficient pattern at various stations in Ethiopia were studied by FAO and classified into fourteen rainfall regimes. The rainfall pattern in the Awash basin reflects the characteristics of four different rainfall regimes i.e., IC (Seven rainy months from March to

September, with peaks in April and August. The coefficients in the intervening months not fall below 1.0.) , IE (Seven rainy months from March to September, generally increasing throughout the period. A high concentration occurs in august (coefficient reaching 3.0).), IIB (Seven rainy months from February to April and from June to September. There is an intervening\g month in which the coefficient falls below 0.6, identifying a bi-modal distribution of rainfall) and IID (Six rainy months being March and April and from June to September. The first peak has coefficient less than 1.0 but there are very high concentrations in July and august, with coefficient greater than 3.0).

The rainfall pattern of the study area is of bi-modal type with most of the rainfall occurring in the wet season (i.e. July-September) and a small rainy season (March-May). The minimum rainfall occurs during the driest months from October to January.

The mean monthly temperature of the study area ranges from 17°C (Bedessa) to 31°C (Gewane). As it is shown on the relationship between mean annual temperature and Elevation the highest temperature observed at the lowest elevation (i.e. at Gewane). The increase of temperature value towards the lowland area reveals that the dryness of the land. The mean maximum monthly temperature of 47°C observed in June at Gewane and in December mean minimum monthly temperate of 2.7°C at Bedessa. The mean annual temperature of the study area is about 25.0°C.

1.3 Geology of the study Area

1.3.1 Regional Geology and Tectonic Setting

The East African Rift System (EARS) is generally considered to be a classic example of a continental rift. The Afar and Ethiopian portions of the rift system comprise the northern 1000km of the EARS. This rift transects the broad Ethiopian plateau, which developed above a Paleogene mantle plume (Schilling, 1992, Figure 1.2).

Recent studies in the Red Sea and Gulf of Aden show that flood basalts were erupted across a ~1000 km diameter region at ~30Ma prior to, or concurrent with, the initiation of rifting

(Menzies et al., 1992). There is little evidence for extension in the Afar/Ethiopian rift, the third arm of the triple junction, until considerably later (at ~18Ma; Gidey WoldeGabriel et al., 1990). Since then the Main Ethiopian Rift has linked northwards into southern Afar and into oceanic spreading in the southern Red Sea (Makris and Ginzburg, 1987)

The Ethiopian rift is a region of sub-E-W extension where extensional velocities (4 mm/yr) are much less than in Afar (20-30 mm/yr) (Bilham et al., 1999). Rift basins are asymmetric, and bounded by steep border faults showing >3 km throw.

The en echelon arrangement of the 'new' magmatic segmentation shows little correlation with the older border fault pattern. Some lavas from the neovolcanic zone show high degrees of crustal contamination, implying localized heating, a hot lower crust, and long crustal-residence times (Schilling et al., 1992); geothermal drilling shows temperatures >350^{o}C at depths of 2 km, with a rapid decrease away from the neovolcanic zone (EIGS, 1987).

Primarily Miocene volcanism occurred on the Ethiopian plateaus flanking Afar, while in Afar volcanism and possibly faulting, began at about 25Ma. Beginning about 4Ma, extensive basaltic volcanism covered most of Afar and obscured the geologic record of events. Since that time, the history of northern and eastern Afar is more a story of sea-floor spreading than continental rifting. While most part of the Alidege surface water catchments area is located within the rift, the eastern extreme part occurs within the eastern Ethiopian plateau. In this area the oldest volcanic rock, mainly basalt known as trap series occurs. These volcanic rocks are voluminous, fissure eruptions dated to be early to mid-Tertiary and mark the initiation of rifting.

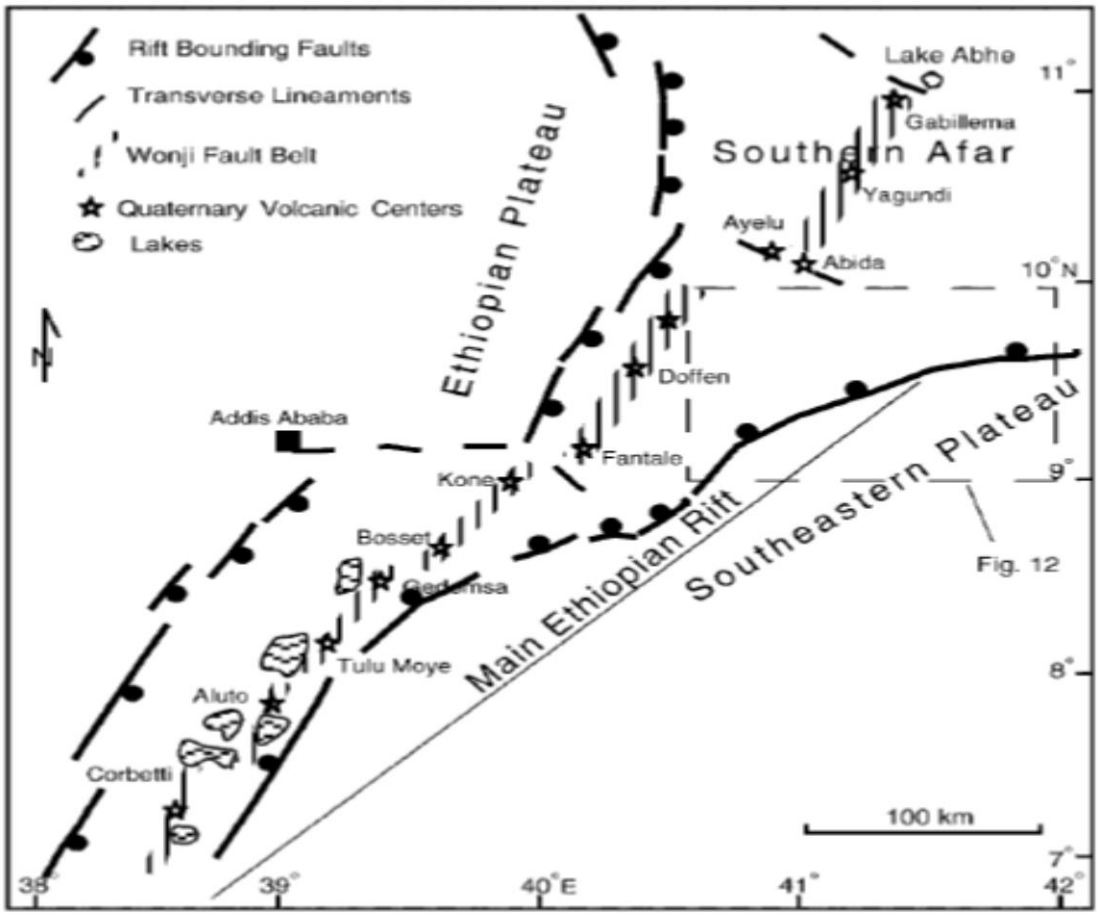

Figure 1.2 Tectonic outlines of the Main Ethiopian Rift and the Southern Afar Rift. The right-stepping Wonji Fault Belt and associated volcanic centers occupy the axial zone of the rift (Tesfaye Korme et al., 2003).

Gidey WoldeGabriel et al., (1990) recognized six episodes of volcanic activity in the main Ethiopian rift starting in the mid-Oligocene or earlier, and they all involve the eruption of transitional basalts. In Afar, volcanism started during late Oligocene-early Miocene (ca. 25Ma) with a second episode in late Miocene (7Ma) and oceanic crust development from Pliocene to present. Magmatism is ongoing and includes historic mafic and felsic lavas - with minor intermediate volcanics - concentrated along faults within the rift axes.

Late Quaternary magmatic segments in the northern Main Ethiopian Rift are separated by narrow fault zones- the Wonji Fault Belt- (Mohr, 1967a, 1967b) and defined by volcanic centers located

within the central rift valleys, including Stratoolcano of Dofan and Shield volcano at Dijilu (See later in III.B). Lavas from these areas comprise the Wonji Group (e.g., Boccaletti et al., 1999; Tesfaye Chernet and Hart, 1999). Pre-Pleistocene volcanism occurred within the same structural segments but outside the modern axial magmatic zones.

Gidey WoldeGabriel et al., (1990); Boccaletti et al., (1999) suggest that the locus of extension and magmatic activity relocated to the narrow axial segments in Pleistocene time, with fissures and small cinder cones becoming active ~1.6Ma.

Most of the geochemical research conducted in this region has surveyed the older Wonji Group lavas outside the modern axial rift (Gasparon et al., 1993; Tesfaye Chernet et al., 1998; Barbieri et al., 1999; Boccaletti et al., 1999; Tesfaye Chernet and Hart, 1999). Investigation of the abundant felsic lavas (which make up >75% of the eruptives) indicate they may be derived by fractionation in shallow crustal reservoirs (Gasparon et al., 1993; Tesfaye Chernet and Hart, 1999), which is consistent with a high degree of underplating beneath the rift axis. Investigations of the mantle source regions of young Ethiopian basalts have documented the presence of at least three components: depleted mantle, Ethiopian lithospheric mantle, and an asthenospheric plume (Tesfaye Chernet and Hart, 1999).

1.3.2 Lithology and stratigraphy

The Ethiopian Rift is an impressive magmatic province on a global scale. It is characterized by largely bimodal magmatism, with transitional basalts that straddle the tholeiitic-alkaline boundary and associated trachyte-pantellerite ignimbrites and lavas. The magmatic evolution of the Ethiopian rift is a key issue to understanding rift processes in general (Menzies, 1992**)**

The crustal extension, which gave rise to the Ethiopian Rift system, also created lines of weakness for volcanic activity. The volcanic activity in the Alidege surface water catchments

area concentrated along these lines of weakness or faults. Not only volcanism that is associated with the fault zones but also series of graben structures occurs in the Southern Afar where alluvial deposits are accumulated. The Alidege plan and Awash basin are contained in a graben structure, which has been partially in-filled with alluvial deposits derived from the near by volcanic terrains.

The lithostratigraphic units in the area are shown on Figure 1.3 and each of these units, starting from the old to the young with their rifting stage is described below

I. Pre-Rift Succession

The evidence of earliest volcanic activity in the Afar region is differentiated by two main episodes of pre-rift flood basalt eruptions (ca. 24 and 10Ma.), which are transitional to tholeiitic in composition.

Alajae Formation

The Alajae formation covering most of the rugged terrain of the eastern water catchments area is grouped as part of the escarpment volcanics or belonging to the volcanic rocks of the Trap series, representing the oldest rock type in the area (Oligocene in age).

Alajae basalt is mildly alkaline to mildly sub alkaline in chemistry, is dominantly aphyric fissural flood basalt with interlayering of rhyolitic lava flows, ignimbrite and rarely trachyte.

Generally the basalt is very fine grained, also locally vesiculated and contain olivine phenocryst. A columnar jointing and strong unsystematic fracturing can be encountered. The basalt is practically impervious except the weathered and fractured zones. The lithologies in this formation are affected by NE-SW and NW-SE trending faults.

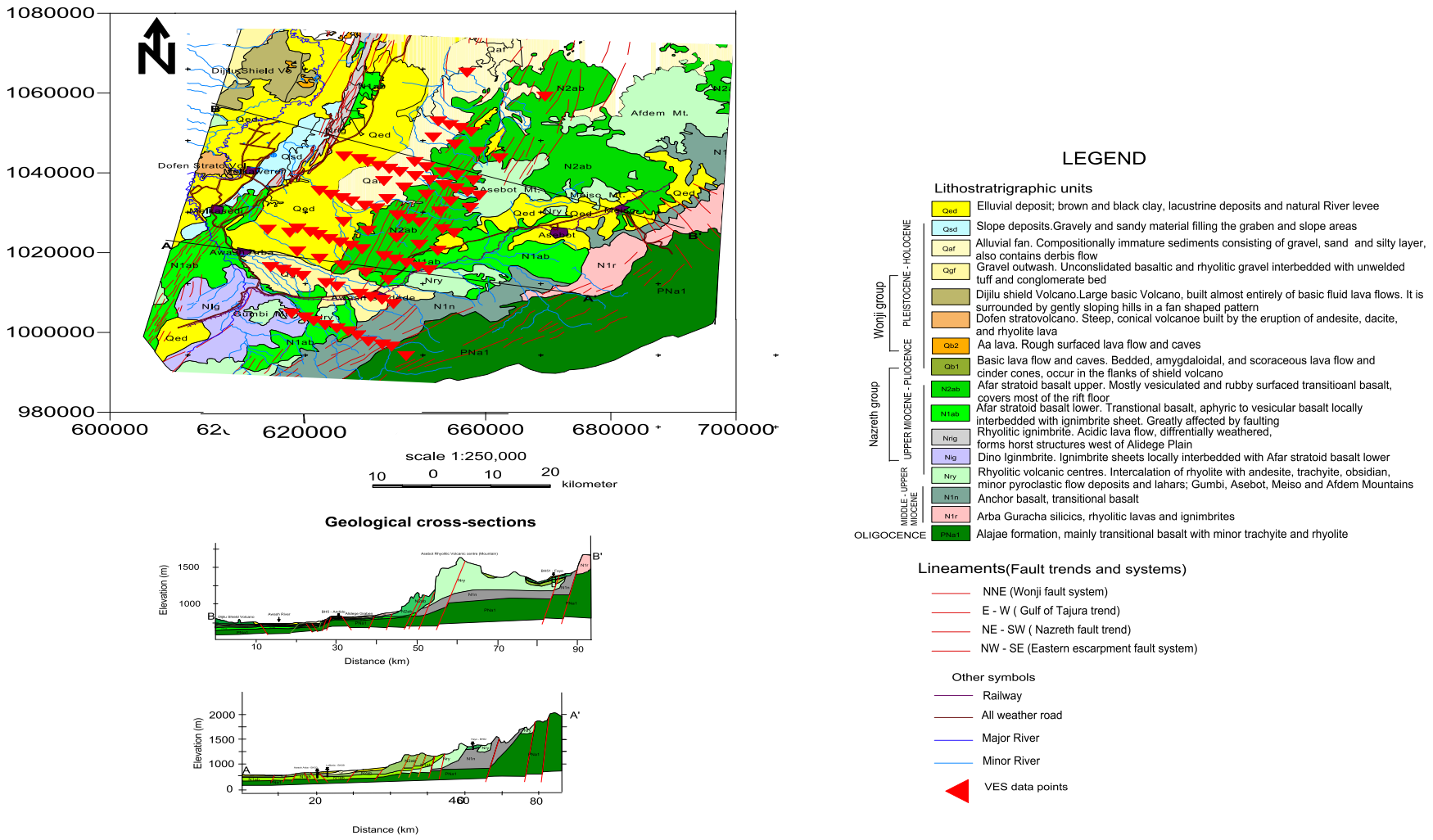

Figure 1.3 Geological map of Alidege Surface water catchments area.

II. Syn-Rift Successions

The close association of stratoid transitional basalts, peralkaline rhyolites and trachytes characterises syn-rift volcanic activity in the Project area. They have erupted along the present-day rift axis of the Wonji Fault Belt (WFB). While the basic rocks are the resultants of outpouring of the upper mantle material, the genesis of acid products can mainly be related to: fractional crystallization from a basaltic parent magma in shallow magmatic chamber ;fractional crystallization plus assimilation of continental crust in crustal reservoirs and during the ascent of mantle melts; and Melting of the continental crust (anatexis) or partial melting of underplated basalts (lower crust).

The main lithologies under this category are:

A. Anchor basalt

This unit is regarded as a product of an early rifting stage and defines the margin of eastern escarpment in the area. It is Mio-upper Miocene in age.

The Anchor basalt outcrops in the east central surface water catchments area. It's grey to dark grey; fine to microcrystalline in texture, fractured and faulted. Fractures and veins in these rocks are in filled with quartz and calcite. The Anchor basalt is transitional in chemistry. The pyroclastic rocks intercalated with the basalt are largely ignimbrite, characterized by homogenous appearance with little sorting of ash particles.

*B. Arba Guracha silicics, rhyolitic lavas and ignimbrit*es

This unit overlies on top of the Alajae basalts, along the eastern margin of the rift. It represents several interlayers of basaltic rocks, rhyolites and ignimbrites.

C. Rhyolitic volcanic centers

This map unit represents rhyolitic domes and volcanic centers of the project area (Asebot, Afdem, Gumbi, Meiso, etc). The unit forms a complex volcano consisting of andesites, trachyites, rhyolites and obsidian. The age of this unit is ~ 7.4Ma. Sharp standing hills, vertical joints with various attitudes are general characteristics. Locally, beds of sinuous and convoluted

obsidian, andesite and rhyolite beds occur and individual beds can be followed for several centimeters.

D. Ignimbrite Sheet

This rock unit is termed Dino Ignimbrite. Ignimbrite sheet covers an extensive area around Awash Sebat Kilo and Gumbi volcanic centre. It is characterised by flows of compact fiamme, in places intercalated with aphyric Afar stratoid basalt and unwelded pyroclastics. The ignimbrite sheet follows valleys and form lower grounds. Locally, reverse grading of large pumice clasts and normal grading of large lithic clasts with fine basal layer is observed.

The ignimbrite lacked internal stratification. At a section, it grades into fine ash deposit consisting of large angular lithic clasts randomly scattered in matrix of low-density pumice and ash. At Gumbi Mountain slope a volcanic mudflow or lahars produced by heavy rain falling on unconsolidated ash has been noted.

E. Rhyolitic Ignimbrite

The Rhyolotic ignimbrite forms a NNE – SSW running horsts (Berita, Nuntiweli, Naleldela, Be-Aditeda, Bilen Ridges, etc*)* between the Alidege and Awash graben. The rhyolitic ignimbrite mantles the topography. The unsorted shards and pumice show close packing, flattening and elongation. The banding seem to be more regular and flatter and close inspection will often show that the individual band is discontinuous and built-up of small often minute fragments some of which show a characteristics and bifurcating shapes of glass shards.

F. Afar Stratoid Basalt (lower)

This unit outcrops in the south central part of the area, in the east around Hardim and low grounds of Asebot Mountain. It forms low-lying hills. The Afar stratoid basalt lower is equal in age to that of the rhyolitic volcanic centers **(**Nry). This unit is massive to vesicular, affected by dominant horizontal jointing and unsystematic dipping joints. This unit is fissural type and

interbeded with ignimbrites. A type area for the intercalating of this basalt with ignimbrite would be the Awash Bridge at Awash Sebat Kilo. The rock unit is greatly affected by major and minor tectonics. Locally this rock unit is very thick, might reach up to 70m, heavily used for quarrying purposes.

III. Post-Rift Successions

*A. Afar stratoid basalt (upp*er**)**

The unit forms both high and low lying hills, conformably overly the lower Stratoid Afar basalt. The Afar stratoid basalt upper is Pleistocene – sub recent in age. The basalt is fine grained massive to strongly vesiculated. The vesicles range from open to being filled by calcite and silica. In the north, around Anegele and Halidebe it is overlain by very recent scoraceous basic and pahoehe lava.

The Afar stratoid basalt upper is transitional in composition (straddle in the tholeiitic-alkalic boundary) with minor under saturated alkaline varieties occurring primarily along the transverse structures of the WFB. The mineral paragenesis in transitional basalts is characterized by olivine, plagioclase and late scarce clinopyroxene phenocrysts; stable olivine and opaques in the groundmass and alkali basalts by olivine, clinopyroxene, opaques and possibly late plagioclase phenocrysts; plagioclase, stable olivine and sometimes alkali feldspar in the groundmass. This transitional basalt marks a change from fissural to central type, covers much of the Afar rift floor.

The basalt is strongly affected by fracturing. Joint type ranges from those of dipping ones following the normal fault trend in the surrounding to those follow the bedding.

B. Recent basic lava

This unit occurs on top of N2ab**,** out crops in Halidebe, Dijilu Shield Volcano in the north and around Dofen Stratovolcano in the East. The basalt is scoraceous and forms both flows and cones, mostly cut by minor faults. The Kone, Buramlore and Webe-Kerdebe cones are entirely

formed of this scoraceous basalt. It is in close association with AA lava and is spread over the surface of NNE trending Wonji fault system in the area.

C. Pahoehe Lava

This unit is a very rough surfaced basic lava flow, out crops in the north, and north east of the project area. It occurs in the vicinity of the scoraceous lava and is the product of both fissural to cone eruptions.

D. Outwash Gravel

Outwash gravel in the area represent Plio – Pleistocene deposits derived from breakdown products of basaltic and acidic materials from the elevated areas, which have been transported towards the centre of the basin to form extensive outwash, gravel plain. The gravel outwash covers extensive areas around cliff faces of Arba River and the surrounding localities, eastern valley sides of Melka Sedi and Amibara. Locally, it is intebeded with basic lava, conglomeratic bed and tuff layer. The outwash gravel contains lenses of clay beds. The clasts are mainly rounded to subrounded indicating a distal source and are mainly of basaltic to rhyolitic type in the unconsolidated finer matrix.

E. Alluvial Fan

The alluvial fan in the area represent a compositionally immature sediments consisting of gravel, sand and silty layer, showing fining direction to the west.

Extensive area east of the Alidege plain, down stream pointes from Asebot volcanic centers contains a fan area of enhanced sedimentation, points where laterally confined flow expands.

F. Quaternary Slope Deposits

Quaternary slope deposits represent a breakdown materials of the elevated areas, consists of mainly sand and gravels - the clasts in the gravel are basaltic and ignimbrite material, seems to be

transported form the near by horsts. The gravel size varies from 10mm-10cm in diameter. The gravel shapes differ from angular to sub-rounded indicating a proximal source. The finer materials are sands and small amount of silt. These slope deposits are transported along minor

stream courses of the region and deposited on the gravel terrace. In some location the material is interblended with the alluvium, especially at the edge of the flood plain traces.

G. Quaternary Elluvium

Quaternary elluvium in the area consists of brown and black clays, sand and silty materials including the lacustrine sediments of the Alidege plain, Melka Werer, Melka Sedi etc. The brown sand, brown silt and clays may represent pre-lake sediment, might have been derived from acidic sequences in the area. The Black clays are confined to a former river system and show cracking and are a product of the break down of the basaltic rocks of the region.

1.4 Hydrogeology

The geological study of the Allaidege plain, which is compiled independently, deals in detail with the stratigraphy and tectonics of the study area. However, the stratigraphy of the plain from to the hydrogeological point of view is discussed below. Figure 1.4 gives the hydrogeological map of the area **(**WWDSE, 2008).

I) Tertiary Volcanoes

- Alaji Formation: This formation covers the south-eastern part of the study area, which is a part of the eastern Ethiopian highland representing the oldest volcanic rock type in the study area. The Alaji formation represents dominantly fissural basalts with inter-layering of rhyolitic lava flows, ignimbrite and rarely trachyte. According to the study of Wabishebele river basin integrated master plan hydro

geological report 2003, the Alaji formation is in general impervious except the weathered and fractured zones.

- Arba Guracha Silicics: It occurs in the extreme south-east study area in high-elevated mountainous plateau and represents basaltic rocks, rhyolite lavas and ignimbrite. No boreholes drilled in this unit so far.
- Anchor Basalt: This unit is outcropped in the extreme south and southern part of the study. Seasonal streams, which drain towards Awash River, emerge from this formation. Fractured and veins in this unit are in filled with quartz and calcite

- Rhyolitic Volcanic centers: This unit represents rhyolitic domes and volcanic centers of the study area (Asebot, Afdem, Gumbi and Meiso). The topographic situation favors quick runoff than infiltration for groundwater.

- Dino Ignimbrite: it is outcropped south of the Alidege plain around Awash Sebat Kilo. Boreholes were not sunk in this unit so far.

- Afar stratoid Basalt: This unit occupies the eastern, southern parts of the study area. It is strongly affected by fracturing. A number of wells are drilled in this unit and it is one of the main water bearing formation around the project area.

II) Quaternary Formations:

- Recent basic lava flow and Pahoehe: These units are outcropped as shield and strato-volcano in some localized eastern and northeastern parts of the project area.

- Alluvial formation: The alluvial formation mainly consists of out wash gravel, Alluvial fan, Slope deposit, and Quaternary Elluvium. It covers large proportion of the western part of Alidege area and considered as the major water bearing formation as a number of productive wells have been sunk into this formation.

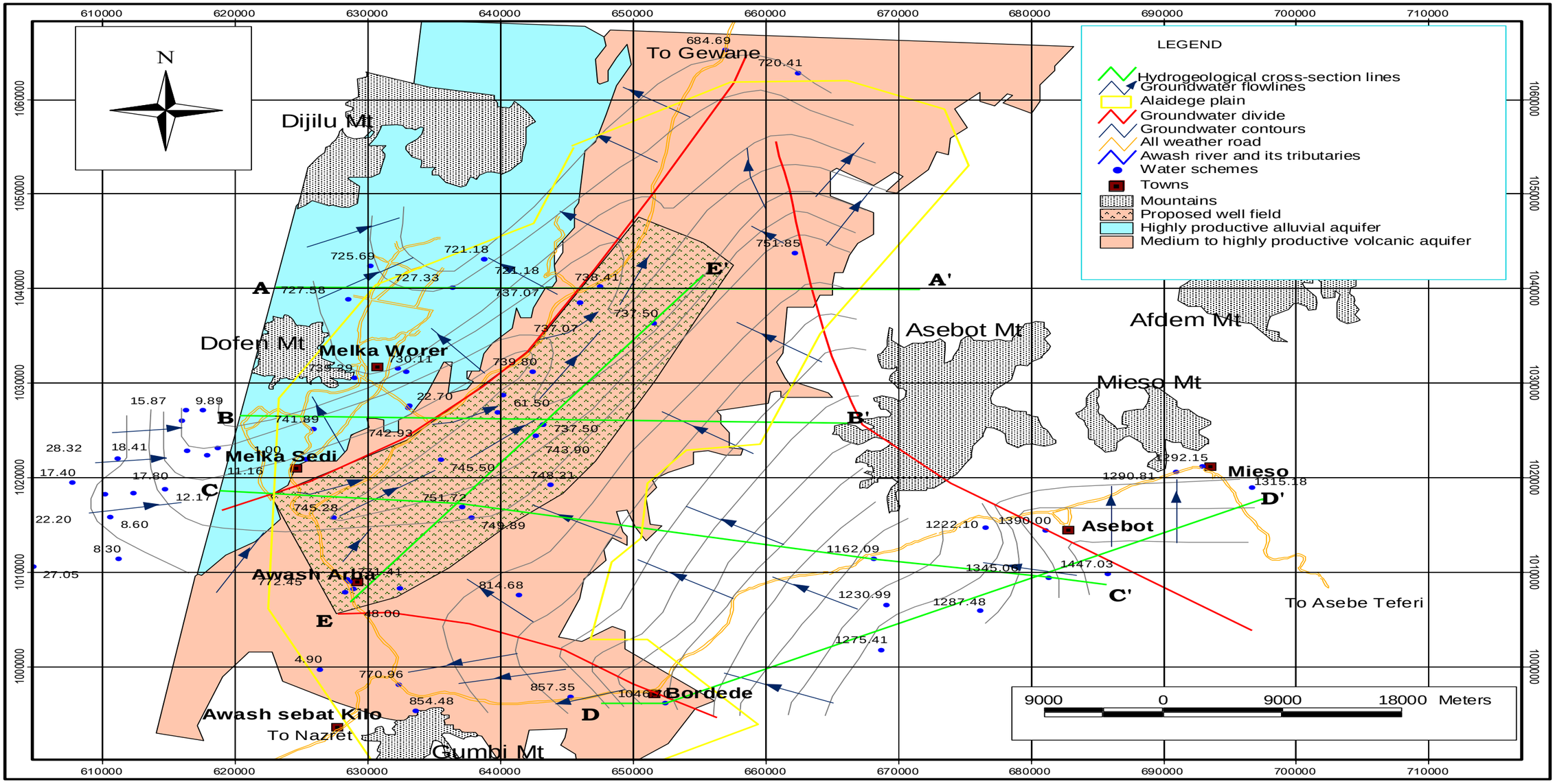

Figure 1.4 Preliminary Hydrogeological map of Alidege plain (WWDSE, 2008)

There exist three ground water divides in the study area; in the southeastern margin of the plain (Asebot area) which is directed NNW-SSE, from Bordered up to Awash arba town along NW-SE direction, and from melka sedi in the NNE direction (Figure 1.4).

In general in the western part the values of the aquifer parameters are significant figures, indicating shallower and higher ground water potential of the area. From the groundwater level map it was possible to identify that the discharge area in the valley are in the far north of the plain.

Table 1.1 gives the list of boreholes that has been sunk in Alidege plain and the surrounding areas. The table also gives essential parameters like transmissivity, drawdown, static water level and well discharge. It is also seen from the table that, the drilling depths of existing boreholes vary from place to place. The depth of shallowest well drilled in the weathered basalt is 37meters deep in the utmost south east of Alidege area, whereas the deepest is 272 meters, drilled in south east of Alidege plain. Average depth drilled in alluvial formation and Basalts is 110 m and 140 m respectively. However, the test well drilled inside the 'Bordede' school has 350m depth which are lowered through volcanics.

Almost all of the wells drilled in the study area are cased by 6 inch steel casing and are used for domestic purpose. The only exception to this is the recently drilled test wells of the area in which 10 inches production casings are used for housing pumps.

1.5 Previous Work

Several geological, hydrogeological, geophysical and engineering geological studies have been conducted in Alidege plain which includes the study area for various purposes. The results of these studies conducted by different authors with different scale includes;- Currey, 1972-1974, discloses that the Awash River discharges water directly into the aquifers under the plain through the areas where the aquifers are exposed along the river (Melka Sedi area). In contrast, the report by Ketema Tadesse and Heroic Ferdinand, 1983**,** Ground water resources study of the Alidege

plain and disagreed with this result and argue that the ground water is transmitted from the surrounding alluvium and the volcanic aquifers to the Awash River.

Table 1.1 Borehole information in the study area.

ID	Borehole Location UTM (m)		Elevation (m above msl)	T in m^2/day	Draw down (m)	SWL	Sp.cap. in l/s/m.	Q in l/sec
	Easting	Northing						
BH-1	627464	1015684	823	6030	1.12	76	44.64	50
BH-2	633633	995257	956	32.9	37.64	101	0.53	20
BH-3	652507	996029	1109	6.75	56.06	65	0.11	6
BH-4	641424	1007510	812	458	3.81	39	1.63	6.2
BH-5	636415	1039961	731	161	26.61	6	1.88	50
BH-6	626003	1025081	814	325	26.41	68	1.29	34
BH-7	635543	1021775	817	119	3.56	5	1.57	5.6
BH-8	643798	1019148	835	34.3	42.6	86	0.38	16
BH-9	642503	1031094	813	60.4	6.5	80	0.85	5.5
BH-10	657056	1065134	840	122	10.7	13	0.59	6.3
BH-11	637170	1016759	830	122	5.06	60	0.99	5
BH-12	645334	996709	1007	10.1	23.26	150	0.17	4
BH-13	645424	996570	824	7.92	89.64	72	0.13	12
BH48	643300	1025542	815	96	7	77	0.79	5.5
BH50	628562	1038760	734	587	1.61	6	3.48	5.6
BH55	632412	998041	892	30.2	10.04	121	0.4	4
BH56	696722	1018866	1382	1910	0.7	67	11.43	8
BH69	681408	1009313	1398	146	4.95	53	1.13	5.6
BH72	685854	1009743	1534	3.58	79.33	87	0.07	5.6

1.6 Statement of the problem

The Alidege plain is situated in the middle Awash basin in Afar Regional State lies between coordinates of 40016'E to 41011'E and 9002'N and 10002'N. Although the geological situation and the low lying and flat nature of the plain, the various streams crossing the plain or ending on it, the structural setting of the area within the Rift favor the accumulation of a considerable groundwater resource within it, no developmental activity has been done so far for the extraction and development of this resource. Therefore, currently there is no supply of water for drinking and any agricultural or economical activity in the plain.

Hence, to investigate the groundwater potential of this vast region, a multi-disciplinary study involving geology, hydrogeology and geophysics has been undertaken by the Ministry of Water Resources through the Water Well Design and Supervision Enterprise (WWSDE) and a good volume of geophysical data of Alidege plain are available. In this thesis work, attempt is made to interpret these set of geophysical data and extract information on the groundwater resource potential of the plain.

The people who live in the study area are mainly nomads except those found near the small towns. They normally travel from place to place, usually for large distances, to look for water and pasture for their cattle. Though the availability of constant water supply is one of the major issues that dictate the settlement of the pastoralist in the area, it is not enough by itself for constant settlement due to the demand for enough pasture. Therefore, the detailed geophysical study for groundwater exploration and hence, the extraction of adequate supply of water is critical thing for the area.

In this thesis work, therefore it is intended to assess the regional groundwater condition of Alidege plain using these set of data.

1.7 Objectives of the study

1.7.1 General Objectives

- The main objective of the study focuses on the assessment and evaluation of the groundwater potential of the Alidege plain and determine the location of preferred borehole sites and the depth at which the aquifers are located.

1.7.2 Specific Objectives

- Identify the major subsurface geological units in the area and map possible water saturated horizons.
- To determine the depth to groundwater table and to locate potential drilling sites for the extraction of groundwater.
- To map the major structures and identify subsurface weak zones that serve as a storage areas or conduits for groundwater movement.

CHAPTER TWO

THEORY OF ELECTRICAL SURVEYS

2.1 General

Geophysics, both solid earth or applied, is the scientific method that uses the science of physics with high degree of technological development employed to observe the hidden earth. In applied geophysics, geophysical methods are developed to delineate the subsurface structure and to explore underground treasures. Nowadays, geophysicists equipped with geophysical instruments, are exploring the deep earth up to several kilometers deep down into the interior of the Earth. Geophysics is not only applied for the subsurface studies but also used to investigate the surface earth, ocean and land of earth, which is the environmental application of geophysics.

Geophysical surveys greatly help in studying the groundwater potential in any hydrogeological setup and locate preferred borehole locations and determine the depth of aquifers. The property and thickness of various lithological units obtained from geophysical survey at different location has been given much attention in part by a desire to reduce the risk of drilling dry holes and also a desire to offset the cost associated with poor ground in groundwater. However, geophysical surveys are not always the most effective method of obtaining the information needed. For example, in some areas drill holes may be a more effective way of obtaining near-surface information than geophysical surveys. In some investigations a combination of drilling and geophysical measurement may provide the optimum cost benefit ratio.

Depending on the source signals, geophysical methods fall into two major groups: those that make use of natural fields of the Earth (passive methods), and those that require artificially generated energy as source signals (active methods).The passive methods utilize the Earth's natural fields which include ;- gravitational and magnetic. The active geophysical methods, in the other hand, involve detection of responses for artificially generated local source fields and waves such as: electrical, electromagnetic and seismic. In general, the aim of geophysical prospecting is searching for local perturbations in the naturally occurring or artificial fields caused by concealed geological features.

Though, almost all geophysical survey methods have wider scope of utilizations, there is always one physical property for which a particular method is exceptionally sensitive and as such determines its specific range of applications. However, a number of geophysical methods may be applied simultaneously (integrated geophysical exploration) in solving certain geological problems, and such approach, greatly reduces the problem of ambiguity, which is the inherent drawback in the interpretations of results from one method, by complementing the information gap from the additional methods. Moreover, surface and drill hole geological information are of vital importance for the successful analysis of geophysical data.

2.2 Electrical Resistivity Method

In geophysical investigations problems such as groundwater exploration, ore prospecting, depth to bedrock determinations, etc., the electrical resistivity method provides a quick and economic means to obtain vital subsurface information. Electrical resistivity methods have been used in a number of groundwater exploration surveys when the resistivities of the rocks are needed to be inferred. The DC-resistivity method measures the potential difference resulted from the artificial excitation due to a current sent to the ground section. The diagnostic parameter, the electrical resistivity ρ, resulting from measurements at a number of electrode positions, reflects the electrical properties in the ground as a function of depth or lateral distance.

The resistivity of the saturated rocks in the upper part of the earth's crust, decreases with increasing their porosity and the degree of salinity of the saturated fluids. In contrary to the above, the presence of clay and conductive minerals can also reduce the resistivity of rocks which can be resolved by using other geophysical techniques, geological or well information. In resistivity surveying especially in vertical electrical sounding (VES), conduction in rocks is mainly due to pore fluids acting as electrolytes. Water in its pure form is poor conductor but most water contains dissolved salts which facilitate current flow.

The resistivity of geological materials exhibits one of the largest ranges of all physical properties from 1.6×10^{-8} Ω m for native silver to $10^{16}\Omega$ m for pure sulphur. According to that range the resistivity of Earth material differ from one another because of the presence of mineralized

zones, zones of water saturation in the subsurface of the Earth. Hence an electrical resistivity method is used to classify the materials due to its properties. (Reynolds, 1997). The theory and basic principle of electrical resistivity method was described by different authors (Telford et al., 1990; Dobrin and Savit, 1976; Parasnis, 1962; Robinson and Caruh, 1988; Reynolds, 1997; Gibson and George, 2003) only a short description of this method is included in this thesis.

2.2.1 Basic Principle of Electrical (DC) Resistivity method

In resistivity method an electric current is introduced in to the ground by means of two current electrodes, and the potential difference between two pair of potential electrodes is measured. The potential difference between two arbitrarily located points on the surface of a homogeneous isotropic ground is obtained from the fundamental given by the expression below.

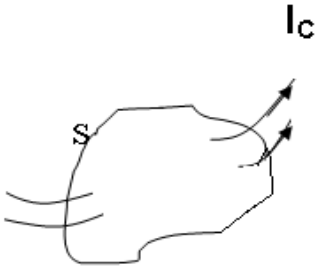

$$(I_c)_s = -\frac{dQ}{dt} \tag{1}$$

$$(I_c) = \oint \vec{J}.ds \quad \textbf{and} \quad Q = \int q.dv \tag{2}$$

where 'v' is the volume bounded by the surface S.

Substituting the above equations into equation (1) and applying divergences theorem, we can get

$$\int_v (\nabla.J)dv = -\int_v \frac{\partial q}{\partial t} \qquad \text{or}$$

(3)

$$\int_v (\nabla . J + \frac{\partial q}{\partial t}) dv = 0$$

Equation (3) is valid for any volume so that we can write it as

$$\nabla \cdot \vec{J} + \frac{\partial q}{\partial t} = 0$$

(4)

Equation (4) is called the law of conservation of charge in differential form and also known as the continuity equation.

For direct current, $\frac{\partial q}{\partial t} = 0$ so that eq (4) reduces to the form

$$\nabla \cdot \vec{J} = 0 \qquad (5)$$

The electric field *E* is conservative field; it can be expressed as a gradient of the scalar potential function V as

$$\vec{E} = -\nabla \vec{V} \qquad (6)$$

where V is measured in volts. From ohm's law; R = V/I, where V and I are the potential difference across the resistor with resistance R (Ω) and the current passing through it respectively. This expression can be written alternatively in terms of the electric field strength E (Volts/m) and the current density (amp/m^2) as

$$\rho = \frac{\vec{E}}{\vec{J}} (\Omega m) \qquad (7)$$

By taking only their magnitudes, the relation between the current density (**J**) and electric field intensity (***E***) can be given as:

$$\vec{J} = \frac{\vec{E}}{\rho} = -\frac{1}{\rho}\nabla V \tag{8}$$

where ρ is a scalar function of the point of observation and *J* is in the same direction as *E* for isotropic medium. From equations (5) and (8) we have

$$\nabla\left(\frac{1}{\rho}\right)\cdot\nabla V + \frac{1}{\rho}\nabla^2 V = 0 \tag{9}$$

This equation is called the fundamental equation of electrical prospecting with direct current.

For homogenous medium, **ρ** is independent of the coordinate axes and equation (9) is simplified as

$$\nabla^2 V = 0 \tag{10}$$

This is called the Laplace Equation for the potential V.

Therefore, the electrical potential distribution for direct current flow in a homogeneous isotopic medium satisfies the Laplace equation. The above equation has different forms in different coordinate systems.

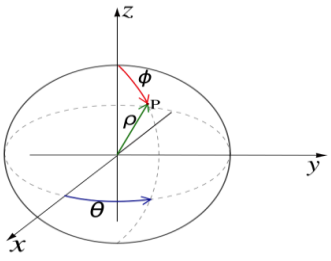

For example, using spherical coordinate system the equation can be expressed as

$$\frac{1}{r^2}\frac{\partial}{\partial r}\left(r^2\frac{\partial V}{\partial r}\right)+\frac{1}{r^2\sin\theta}\frac{\partial}{\partial\theta}\left(\sin\theta\frac{\partial V}{\partial\theta}\right)+\frac{1}{r^2\sin^2\theta}\frac{\partial^2 V}{\partial\phi^2}=0 \quad (11)$$

Practically, the DC resistivity survey is conducted with two current electrodes (AB) called source and sink respectively, in which the current I (A) is injected in to the ground and two potential electrodes (MN) where the potential difference ΔV (V) is recorded.

If one considers (DC) source which delivers current I(A) to the homogenous, isotropic earth through the current electrodes, the potential at any point will vary as a function of r where r is the distance from the ground to the current electrodes.

Let us now suppose that a current I be introduced in to an infinite homogeneous medium at a point P. then the potential at a distance r from p will be a function of r and hence Laplace equation can be written as

$$\frac{d^2V}{d^2r}+\frac{2}{r}\frac{dV}{dr}=0 \quad (12)$$

Since the potential varies only as a function of r, $\frac{\partial V}{\partial\theta}$ and $\frac{\partial V}{\partial\phi}$ will be zero.

Current is introduce into the ground by means of two electrodes, i.e., a source and sink; and the potential at any point due to this "bipolar "arrangement is

$$V=\frac{I\rho}{2\Pi}\left(\frac{1}{r_1}-\frac{1}{r_2}\right) \quad (13)$$

where r_1 and r_2 are the distance of the point from the source and the sink, respectively.

Consider that a direct current of strength I is introduced in to a homogeneous and isotropic earth by means of two point electrodes as shown in the Figure 2.1. The potential difference between the two points P_1 and P_2 on the surface is given by using equation (12) as

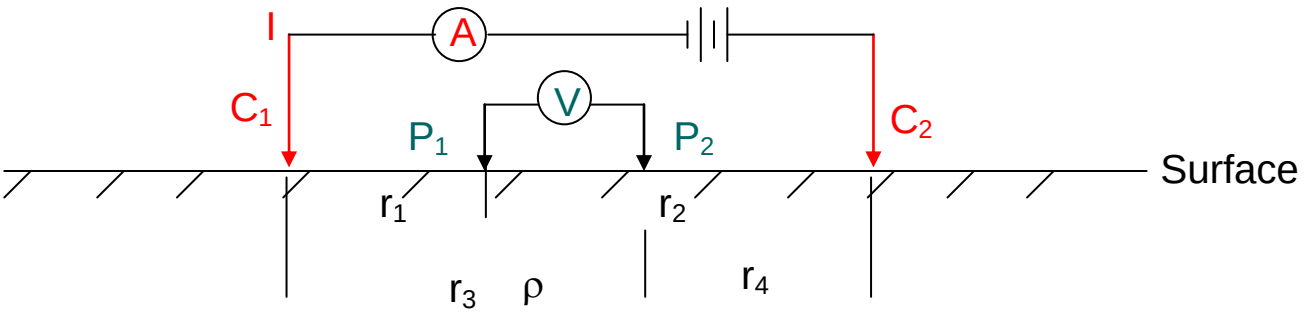

Figure 2.1 The arrangement of current and potential electrodes in a four-electrode system.

The potential at P_1 $$V_{p_1} = \frac{I\rho}{2\Pi}\left(\frac{1}{r_1} - \frac{1}{r_2}\right)$$

Similarly the potential at P_2 $$V_{p_2} = \frac{I\rho}{2\Pi}\left(\frac{1}{r_3} - \frac{1}{r_4}\right)$$

The potential difference

$$\Delta V = \frac{I\rho}{2\Pi}\left(\frac{1}{r_1} - \frac{1}{r_2} - \frac{1}{r_3} + \frac{1}{r_4}\right) \qquad (14)$$

where the distances r_1, r_2, r_3 and r_4 are all in meters.

Therefore, after re-arranging the distances between the current and potential electrodes according to the well known configurations, we can determine the resistivity of the homogenous ground.

2.3 The Apparent resistivity

If the ground is homogenous, the potential difference measured is as a function of the true resistivity of the homogeneous earth and the geometric factor. But in reality the ground is locally in the homogeneous and the potential difference depends on the current applied, the resistivity of the sub surface medium and the geometrical factor (k) determined by electrode array or configurations types. The resistivity calculated from such non homogenous ground is not a true resistivity rather it is called apparent resistivity (ρ_a) which can be related to the parameter as

$$\rho_a = k\frac{\Delta V}{I} \tag{15}$$

This apparent resistivity has to be interpreted using curve matching or inversion techniques to find estimated resistivity versus depth of the subsurface.

This are many type of electrode configurations used in ground surveys of which the most commonly used array are Wenner, Schlumberger and the Dipole-Dipole. Since the electrode separation relate to the investigation depth and lateral solution power required, one can choose the best electrode configuration for his planed survey at the initial of his survey .the expression for apparent resistivity in each of the above array types will be different due to the difference in the geometrical factor (K) of each any types.

Take the Schlumberger array in which the electrodes are symmetrically placed a point at the center of the array as shown in the figure below.

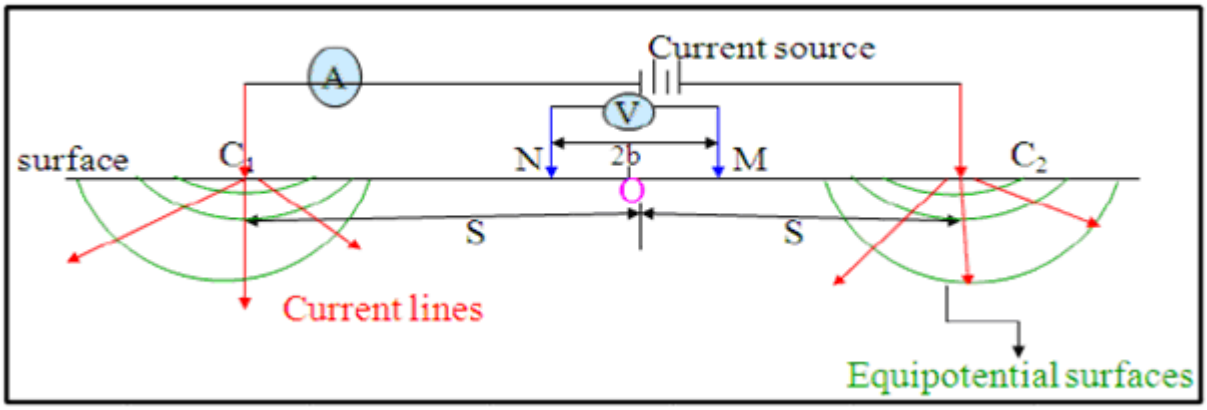

Figure 2.2 The electrode arrangement for the Schlumberger Array.

where $r_1 = s - b_1$=s-b, $r_2 = s + b$, $r_3 = s + b$ and $r_4 = s - b$, 'O' is the center of the array.

The potential difference ΔV using eq (14) is given by;

$$\Delta V = \frac{I\rho}{2\Pi}\left[\left(\frac{1}{s-b} - \frac{1}{s+b}\right) - \left(\frac{1}{s+b} - \frac{1}{s-b}\right)\right]$$

$$\Delta V = \frac{I\rho}{2\Pi}\left[\left(\frac{1}{s^2 - b^2}\right)\right] \tag{16}$$

$$\rho_a = \Pi\left(\frac{s^2 - b^2}{2b}\right)\left(\frac{\Delta V}{I}\right) \tag{17}$$

where the geometric factor

$$k = \pi\left(\frac{s^2 - b^2}{2b}\right)\left(\frac{\Delta V}{I}\right) \tag{18}$$

2.2.2 Resistivity Sounding Principle

In resistivity sounding, which is also know as Vertical Electrical Sounding (VES), the positions of electrodes changed with respect to a fixed point (known as the sounding point) and the measured values reflect the vertical distribution of resistivity values on a geologic section.

Vertical electrical sounding (VES) consists of a symmetrical electrode array used to determine the resistivity of the subsurface which is assumed to be horizontally stratified layers. The procedure is used to determine the variations in resistivity in the vertical direction and called electrical drilling or commonly vertical electrical sounding (VES). By expanding symmetrically the distance between current electrodes about a point called the sounding point, while keeping

the potential electrodes MN at the same position, provides a sounding curve corresponding to the apparent resistivity versus depth of the location. As the spacing between the current electrode increases, the investigated depth will also increase.

The two most commonly used arrays in electrical sounding survey are the Wenner and Schlumberger arrays. In this work, we have used the data which was collected by using the Schlumberger electrode array techniques. When the Schlumberger array is used, the distance between the potential electrodes is not greater than one tenth of the current electrodes spacing.

The advantage of this array is that initially only the spacing between the current electrodes is increased. However, at large current electrode spacing, the measured potential becomes very low and the distance between the potential electrodes is increased. Increasing the potential electrode spacing produces a 'step' in the apparent resistivity curve and it is good practice to obtain an overlap between the curve segments by obtaining two readings at different potential electrode spacing for two adjacent current electrode spacing. Segments obtained at larger potential electrode spacing can be shifted in order to produce a smooth curve (Gibson and George, 2003).

In electrical prospecting to determine the depth and the electrical resistivity of a series of horizontal or nearly horizontal ground. In order to solve this problem, we should calculate the potential and the electric field, due to a point source of current, at any point on the surface of a stratified earth. This has advantages because of enables one to use axial symmetry of the potential filed about the vertical axis through the current source and the additive ness of the potential is also be used.

Let as choose a cylindrical system of coordinate with the origin at the point source a direct current located on the surface. The subsurface consists of infinite number of layers separated by horizontal boundary planes, the deepest layer existing to infinite depth ($h_n \to \infty$) and the other layers have finite thickness

h_i = h1, h2,h3…h_n and resistivities ρ_1, ρ_2, ρ_3, …ρ_n. Each of the layers is electrically homogeneous and isotropic.

The derivative of the potential based on the above conditions was first due to Steanescu et al., (1930).

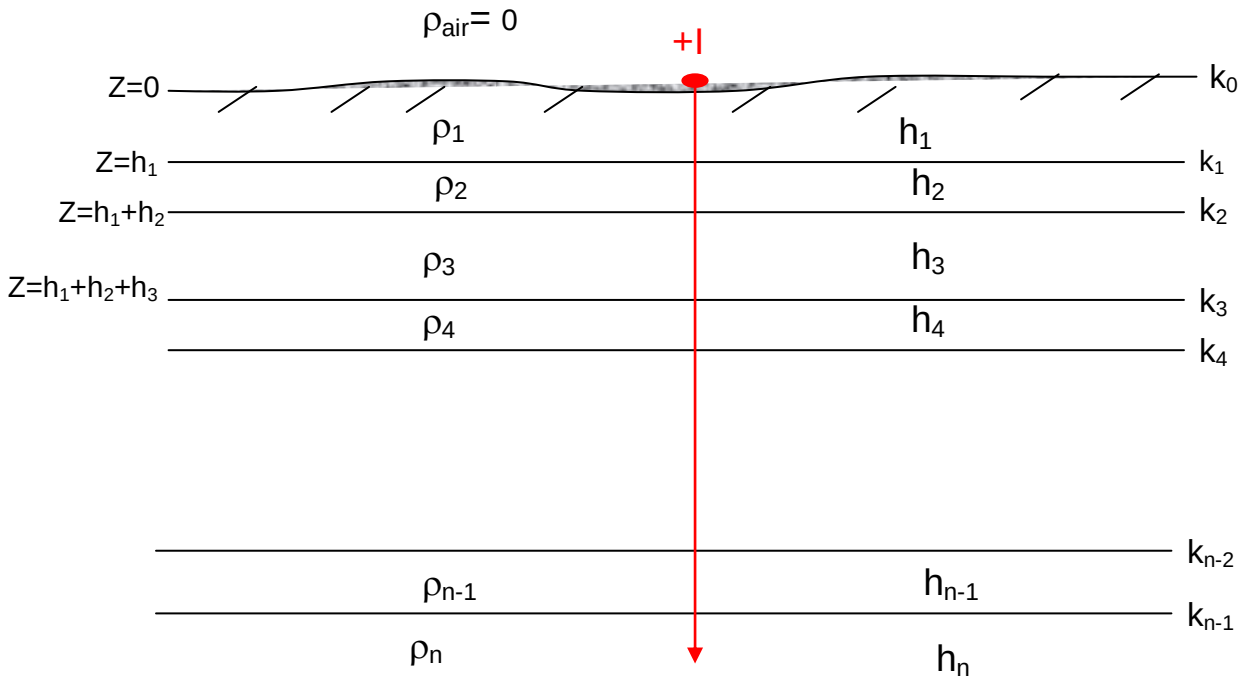

Figure 2.3 A multi-layer Earth and problem presentation for solution of the potential.

The electrical potential field V for direct current satisfies the differential equation of Laplace, Which is

$$\frac{\partial^2 V}{\partial x^2}+\frac{\partial^2 V}{\partial y^2}+\frac{\partial^2 V}{\partial z^2}=0 \qquad (19)$$

The potential field has a cylindrical symmetry with respect to the vertical axis line through the current source .therefore, Laplace equation in cylindrical coordinate is most appropriate.

For a solution symmetrical with respect to the vertical axis $\frac{\partial V}{\partial \theta}=\frac{\partial^2 V}{\partial \theta^2}=0$ so,

$$\frac{\partial^2 V}{\partial r^2}+\frac{1}{r}\frac{\partial V}{\partial r}+\frac{\partial^2 V}{\partial z^2}=0 \tag{20}$$

The particular solution of equation (20) can be obtained using the method of separation of variables and can be assumed to be of the form

$$V(r,z)=U(r)W(z) \tag{21}$$

Substituting equation (21) to (22) and dividing throughout by the product U(r) W (z) gives

$$\frac{1}{U(r)}\frac{d2U(r)}{dr2}+\frac{1}{rU(r)}\frac{dU(r)}{dr}+\frac{1}{W(z)}\frac{d2W(z)}{dz2}=0 \tag{22}$$

This equation is satisfied if and only if

$$\frac{1}{U(r)}\frac{d2U(r)}{dr2}+\frac{1}{rU(r)}\frac{dU(r)}{dr}=\lambda^2 \tag{23}$$

and

$$\frac{1}{W(z)}\frac{d2W(z)}{dz2}=-\lambda^2 \tag{24}$$

where λ is an arbitrary constant.

The solution of equation (24) may be given as

$$W(z)=c_1e^{-\lambda z} \quad \text{and} \quad W(z)=c_2e^{+\lambda z} \tag{25}$$

and that of equation (24) is given as

$$U(r) = c_3 J_o(\lambda r) \tag{26}$$

Where Jo is the Bessel function of order zero

The combination of equation (25) and (26) gives the particular solution of the deferential equation given by equation (20), which is

$$V(r,z) = c_5 e^{+\lambda z} J_o(\lambda r)$$

and $$V(r,z) = c_5 e^{-\lambda z} J_o(\lambda r) \tag{27}$$

where c and λ are both constants in the last of these equations.

Since, by theory of differential equation, every linear combination of the particular solution is also a solution, one can make λ to rough all possible values from 0 to ∞ and allowing the constant "c" to very independence of λ the general solution of equation (21) can be obtained as

$$V(r,z) = \int_0^\infty \left[\Phi(\lambda) e^{-\lambda z} + \Psi(\lambda) e^{-\lambda z}\right] J_o(\lambda r) d\lambda \tag{28}$$

Here $\phi(\lambda)$ and $\Psi(\lambda)$ are arbitrary functions of .the boundary conditions control the special form of these equations .From the basics theory, the potential generated by a single point source of current intensity "I" located at the surface of an electrically homogeneous earth is given by

$$V = \frac{I\rho}{2\pi} \frac{1}{\sqrt{r^2 + z^2}} \tag{29}$$

where ρ is the resistivity of homogeneous Earth.

Equation (29) can be written in integral form by using the so-called Lipschitz integral (also called the Weber Integral Formula) in theory of Bessel function as

$$\int_0^\infty e^{-\lambda z} Jo(\lambda r) d\lambda = \frac{1}{\sqrt{r^2 + z^2}} \tag{30}$$

So that equation (30) gives

$$V = \frac{I\rho}{2\pi} \int_0^{\infty} e^{-\lambda z} Jo(\lambda r) d\lambda \qquad (31)$$

Equation (31) is also a solution of equation (20). Therefore, the combined solution will also be a solution to the equation, that is

$$V(r,z) = \frac{I\rho}{2\pi} \int_0^{\infty} [e^{-\lambda z} + \Theta(\lambda) e^{+\lambda z}] Jo(\lambda r) d\lambda \qquad (32)$$

where θ(λ)and χ(λ) are arbitrary function λ. Solutions of equation (32) are valid in all the layers of the subsurface. However, necessarily the same in the different layers of the subsurface .therefore, the potential due to a point source of current at the surface of a horizontally layered earth must in each layer satisfy

$$V_i(r,z) = \frac{I\rho}{2\pi} \int_0^{\infty} \begin{bmatrix} e^{-\lambda z} + \Theta_i(\lambda) e^{+\lambda z} \\ + \mathrm{X}_i(\lambda) e^{+\lambda z} \end{bmatrix} Jo(\lambda r) d\lambda \qquad (33)$$

This equation is called the Stefanescu Integral, with **I** referring to the several layers of the subsurface.

Boundary conditions

For a potential set up by a single source of current at the surface of a horizontally stratified earth

1. At each of the boundary planes in the subsurface, the electrical potential must be the same $V_i = V \ldots$ at $Z = h_i$ (34)
2. The vertical component of the current density must be continuous on each boundary plane (the current density normal to the boundary planes …)

$$(J_i)_N = (J_{i+1})$$

$$\frac{1}{\rho_i}\frac{\partial V_i}{\partial z} = \frac{1}{\rho_{i+1}}\frac{\partial V_{i+1}}{\partial z} \qquad (35)$$

3. At the surface (z=0) the vertical component of the current density Jv (and hence that of the electric field intensity) must be zero everywhere except in the infinitesimal neighborhood around the current source. (in air $J_{air} = 0$ and from condition (2), the vertical component of the current density at depth zero must be zero).near the current source the potential must not approach infinity (must remain finite) as

$$V = \frac{I\rho}{2\pi}\frac{1}{\sqrt{r^2 + z^2}}$$ at depth 0, Z =0, as r → 0

4. At infinite depth, the potential must approach zero, i.e. V → 0 as Z→ ∞

CHAPTER THREE

DATA ACQUISITION, PROCESSING AND PRESENTATION

3.1 General

The choice of geophysical techniques for subsurface investigations should be made judiciously as their success depend, largely, on their suitability to the problem, among other factors. Certain problems are best solved by a particular method than other and thus, require serious consideration. However, the local terrain conditions, access and logistic difficulties, and most importantly availability of instruments and associated cost, impose further constraints on this difficult task.

In light of the above mentioned considerations, potential filed methods, namely electrical resistivity technique using Vertical Electrical Sounding (VES) are appraised to achieve some of the objectives of the research work.

3.2 Instruments

The instruments used in the resistivity survey consisted of a portable integrated resistivity meter OYO MCOHM Mark-2, Model 2115A powered by GS 60 AH, 12V battery together with other accessories such as interconnecting cables with reels and electrodes.

The Schlumberger electrode configuration was used for the Vertical Electrical Sounding measurements in all the investigated sites, with the maximum half-current electrode separation used varying from sounding to sounding depending on the local conditions, but generally in the range of 500m to 1000m.

3.3 Data Acquisition

A total of ninety sounding data were used for this thesis work, which are obtained from the Water Works Design and Supervision Enterprise (WWDSE). The location of these VES and their distribution on Alidege plain is given in Figure 3.1. For each VES, the symmetrical

Schlumberger electrode configuration was used for all soundings. The maximum current electrode separation, (AB/2) =1000m, was chosen based on the depth of interest, (the anticipated depth to the water bearing horizon) and subsurface geology.

In each case, the sounding curve, which is a log-log graph of apparent resistivity versus half the current electrodes separations, was plotted, right in the field as a measure quality control. If any error is detected during data acquisition, it was automatically corrected either by taking repeated measurements, by improving the contact resistance of the electrodes or by changing the position of the measuring electrodes.

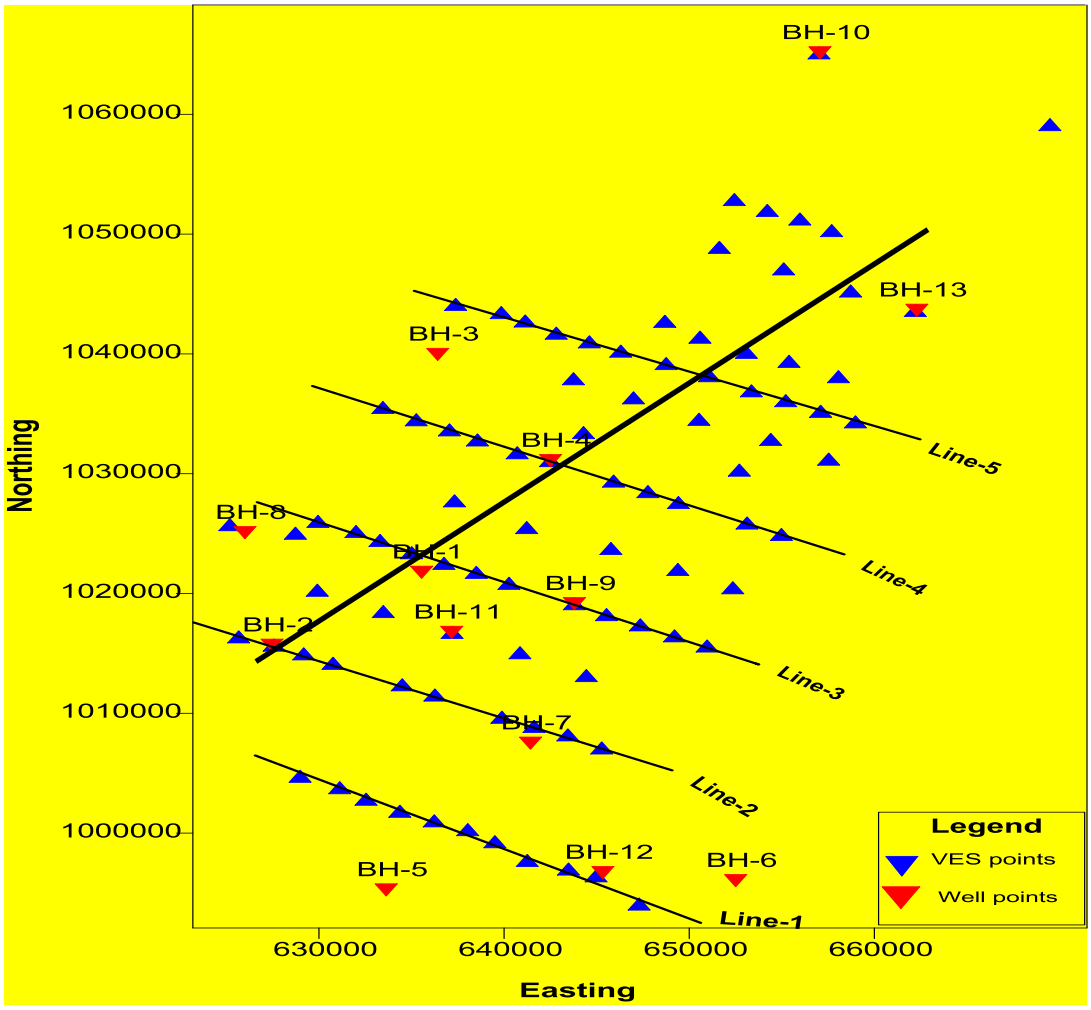

Figure 3.1 Location of the vertical electrical sounding (VES) points.

3.4 Data reduction

The apparent resistivity values are plotted on logarithmic transparent paper. In processing of the collected data, the apparent resistivity value on the ordinates and the electrode separation (AB/2) on the abscissa. The resistivity measurements were made by progressively increasing the potential electrode distance (MN) for relatively large increment of the current electrode distance (AB/2). In most cases the sounding curve is segmented due to overlap measurement and can not be interpreted as it is. To have precise interpretations the segmented curves were shifted to the small MN curve points, so that the effect could be quantified and corrections could be made in order to obtain a single smooth curve that could be processed with the computer using "RESIXIP" software (Velpen, 1995)

3.5 Data processing and presentation

The electrical sounding data collected in the field work were plotted on a bi- logarithmic paper and interpreted by using two layer master curves and auxiliary charts to find out initial model parameters for the thickness and electrical resistivity of the possible layers mapped with survey. These parameters obtained from curve matching techniques arranged and analyzed with litho logical units of existing boreholes were used as initial model in the WIN RESIST inversion software which resulted in improved and reliable electrical parameters under the area of investigation as depicted in the interpreted sounding resist curves. Consequently, from the results of these interpreted geoelectric parameters. The depth, thickness and resistivity parameters acquired by the mentioned software program of vertical electrical sounding curves were used to construct geoelectric sections for each VES to show the distribution of different lithological unit in vertical direction using the software AutoCAD, 2007 programs.

Geoelectric Sections are constructed according to the traverses they positioned. Available lithological logs from boreholes in proximity of the surveyed traverses have been used for calibration and further refining the results. Thus, interpreted VES points at existing well sites are employed for calibrating the sounding points with in the area.

Principle of Equivalence and Suppression

The principle of equivalence and suppression introduce ambiguity and a non-unique solution in electrical resistivity interpretations. Equivalence refers to the condition in which different combination of layer resistivity and thickness may lead to apparent resistivity curves, which are within the accuracy of observation. As well as these curves are indistinguishable although not identical.

Whereas suppression refers to the condition in which the effect of an intermediate layer (thickness very small compared to its depth) in apparent resistivity curve of ascending and descending type is small that its detection from the curve may be impossible.

There are different types of equivalence:-

1) For $h_2 < h_1$, $\rho_2 < \rho_1$ and $\rho_3 > \rho_2$, theoretical computation of the potential for a three layer section shows that, the result does not depend on the individual values of the parameters of the intermediate layer but only on the ratio $h_2/\rho_2=S$. This is referred to as H-type equivalence i.e., if the resistivity and thickness of the intermediate layer are changed within a certain range, keeping the conductance (=conductivity x thickness) constant, the observed apparent resistivity curve remains invariant, within the acceptable margin of observational error. Since both H- and A- type sections satisfies the condition that $\rho_3 > \rho_2$, they may be called equivalent with respect to S.
2) For $h_2 < h_1$; $\rho_2 >> \rho_1$ and $\rho_3 < \rho_2$, the value of the potential depends only the product $h_2 \rho_2 = T$. This is referred to as K-type of equivalence in which the shape of the curve remains invariant as far as the transverse resistance, T, is kept more or less constant. And, as both K- and Q- type sections satisfies the condition that $\rho_3 < \rho_2$, they may be called equivalent with respect to T.

CHAPTER FOUR

RESULTS, DISCUSION AND INTERPRETATION

4.1 General

The apparent resistivity data and the interpreted layer parameters of each sounding curve were used to produce different anomaly maps which show contrast in the resistivity and depth of the subsurface rocks. These presentations include apparent resistivity pseudodepth sections, sliced-stacked sections and geoelectric sections. The apparent resistivity depth sections were plotted using the raw data while the geoelectric sections were constructed after the data from each of the sounding points have been interpreted separately and the resistivity and thickness of the subsurface layers beneath the sounding points have been determined.

For this purpose preferential lines, where a number of sounding points are found to be aligned, were chosen over which the sections are to be constructed. From the total of 90 VES, it was found possible to choose 5 parallel lines and one cross line on which adequate number of VES are located to construct a realistic section of the ground.

These sections and the data from the aligned VES were used to study the variations in resistivity of the subsurface rocks. The plots of pseudodepth (on the selected line) and apparent resistivity sliced pseudo depth map of the study area give a general picture on the variation of the resistivity with depth over the area, while the geoelectric sections are the results of interpreted true resistivity parameters of the subsurface and are believed to represent the subsurface electrical stratification more realistically.

A combination of software has been used for the purpose: RESIXIP and WinResist softwares (Velpen, 1995) for interpretation of the individual VES, Surfer (version Surfer 9.1) software (Golden software, 2010) for plotting the pseudodepth and sliced depth sections and the AutoCAD plotting software to construct the geoelectric sections. In the following sections we present these sections and discuss them separately.

4.2 Sliced-Stacked section

The apparent resistivity sliced pseudodepth map shown in Figure 4.1 is prepared by superimposing the two dimensional apparent resistivity plan maps for six different half-current electrode spacing. All the VES (88 of them) except two sounding are used for qualitative assessments of the electrical nature of the geologic medium. The sounding points are not evenly distributed and they are mainly concentrated on the central part of the area, but their large numbers and wide coverage is still believed to give a good representation of the ground overall. The spacings chosen for this representations are AB/2= 45, 150, 330, 500, 750 and 1000 m and are believed to be adequate to represent the variation in apparent resistivity over the whole surveyed area with depth.

Specifically, the map (Figure 4.1) shows the relative variation of the apparent resistivity value of the whole area laterally as well as vertically at different pseudo depths. It is found that the apparent resistivity value varies considerably from 2-322 Ohm-m.

According to Figure 4.1 the most interesting feature of this sliced plot is the low resistivity zone, (< 42 Ω-m) that occupies the vast portion of the survey area. The value of the high apparent resistivity value zone decreases as the investigation depth increase. The value of the low apparent resistivity zones observed in the northeast and southwest parts of the area increases as depth increases.

On the other hand, the relatively very high resistivity response, (>160 Ω-m) that is found in northeast and high resistivity response, (>62 Ω-m) that is found in south part at AB/2=45m and AB/2=150m. However this high resistivity zone decreases with depth and finally low resistivity zone dominates at and beyond AB/2=750m.

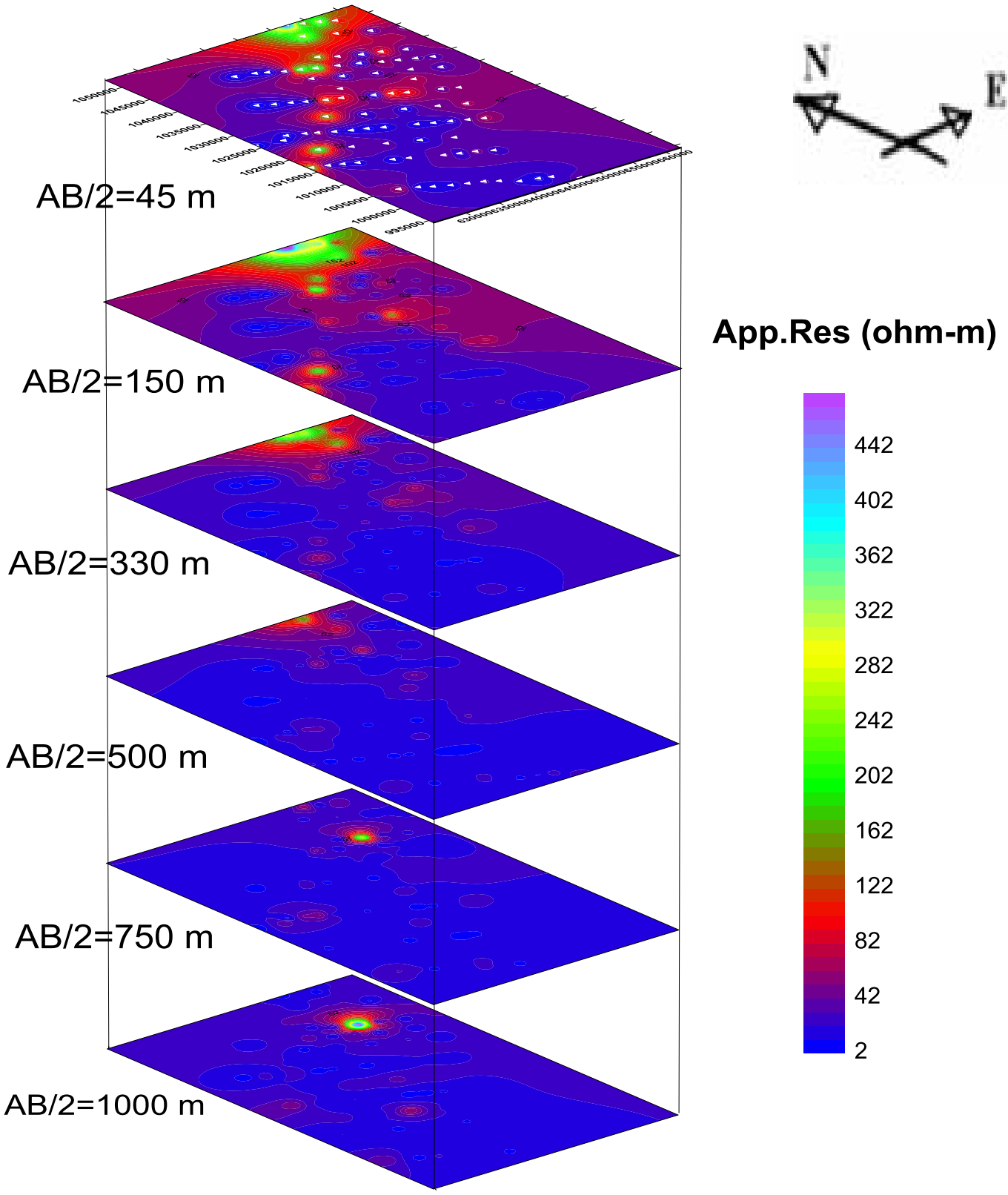

Figure 4.1 Stacked apparent resistivity section of Alidege plain.

4.3 Apparent resistivity Pseudodepth and Geoelectric sections along the selected Lines

From the total of 90 VES, it has been possible to select a number of VES that are well aligned to enable us to construct pseudodepth and geoelectric sections. To this end, 5 parallel lines (Lines-1 to Line-5) and a cross profile line Line-6) were chosen. The number of VES on each line and the designation of the VES are given in the following table:

Table 4.1 VES points on each line and its length.

Line No	VES points lying on the traverse Line	Line length (km)	Remark
1	VES-99, 98,97,96,95,94,93,92,91,90 and VES-100	21.5	
2	VES-1,2,3,4,6,7,9,10,11 and VES-12	21.7	
3	VES-25,24,23,22,21,20,19,17,16,15,14 and VES-13	23.5	
4	VES-26,27,28,29,30,31,33,34,35,37 and VES-38	24	
5	VES-39,40,41,42,43,44,84,48,49,50 and 51	23.8	
6	VES-55,73,71,85,65,32,31,45,23,5 and VES-1	47	Cross section line

On the average, the VES on each line are found to be spaced at 2.5 km, and the average data density over the whole area is 18.7 VES points/km^2 and this spacing is adequate for regional groundwater potential studies for such a vast area.

The apparent resistivity pseudodepth section along the selected lines are mapped from raw data using surfer software and the resistivity sounding geoelectric sections along the selected line are

constructed from the interpreted layer parameters of each VES points (sample interpretations of the individual VES are shown in Annex-1). In interpreting these field curves, a combination of RESIXIP and WinResist software were used. The initial model parameters were obtained using the RESIXIP interactive software and 1X1D software. These model parameters were then used to invert the field data. Optimal RMS error of less than 4 has been taken to be acceptable.

In the following sub sections, the apparent resistivity pseudodepth and geoelectric sections for each line are presented and discussed separately.

4.3.1 Traverse Line-1

This line is on the southwestern most end on the Alidege plain and is oriented in near north west to south east direction. The line has a total length of about 21.5 km and there are 11 VES (VES points 99, 98…100) with average VES point spacing of about 2 km.

A. Pseudodepth section along Line-1

The pseudodepth section constructed for the 11 VES that lie on the survey traverse Line-1 are given in Figure 4.2. According to this figure, there is a distinct lateral variation in resistivity in the top most part of the section with prominent high resistivity top zones mapped around VES-92, VES-97, VES-96, VES-99 and VES-100. This high resistivity zone is found to extend to large depth only in the region around VES-99, and to some extent around VES-100. Otherwise, the vast region under the section shows extensive coverage of the low resistivity zone. The resistivity ranges (0 to 33 Ohm-m) of this low resistivity region are indicative of potential water saturation, with the need to closely look into the possibility of this low resistivity resulting from higher mineralized/ higher salt concentration groundwater.

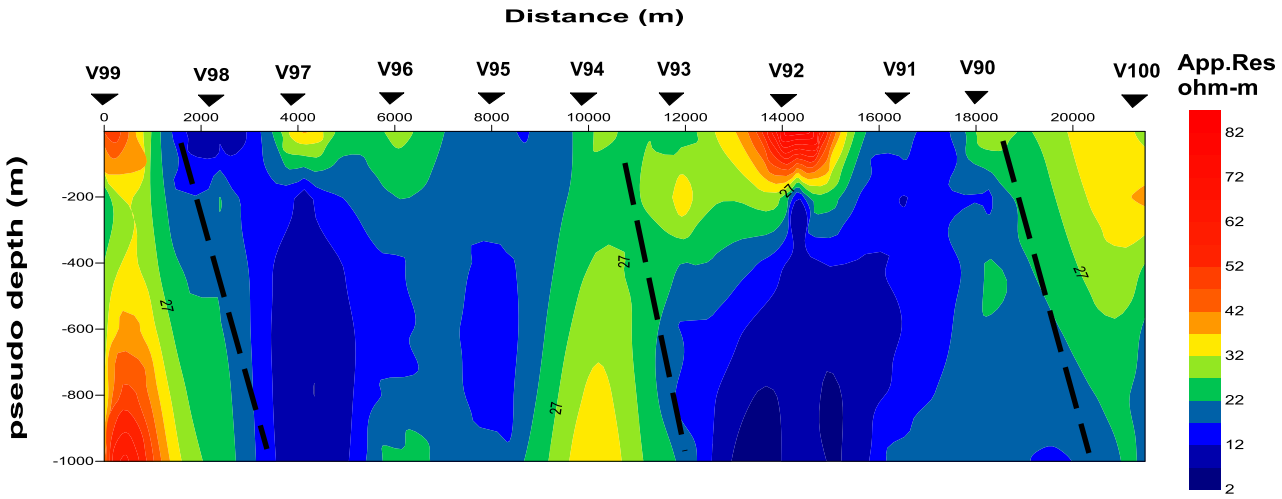

Figure 4.2 Pseudodepth sections along Line-1, Alidege plain.

B. Geoelectric section along Line-1

The resulting geoelectric section constructed from the interpreted layer parameters of the 11 VES lying on this traverse is given in Figure 4.3. A borehole BH-12 is located near Line-1; especially close to VES-90 was also used to constrain depth and identify the lithological units beneath these VES points during modeling. In essence, the lithological description of the borehole depth section (given in Annex 2) with their resistivity parameters from each interpreted VES were used to prepare the geoelectric section shown below (Figure 4.3).

From the section given in Figure 4.3, it is seen that the subsurface consists of 4-5 geoelectric horizons. The layer representing the top part of the section, which is difficult to represent with the given scale, consists of two-three layers whose resistivity values show large lateral variations. These variations are believed to result from either difference in lithology or soil moisture content. Beneath these layers is a relatively low resistivity horizon (25 to 47 Ohm-m), scoraceous basalt covering the region from the center of the line towards SE direction. Its thickness extends from a depth of about 10 m to about 60 m on the average with the layer becoming thick (100 m) around VES-100. The low resistivity response of this layer shows that it is possibly water saturated. Towards the north western side of the line, the resistivity values suggest the presence of a structure somewhere between VES-97 and VES-98 as well as VES-95 and VES-96. Specifically, on the northwester side of the line there is a high resistivity zone extending to a depth of about 60 m.

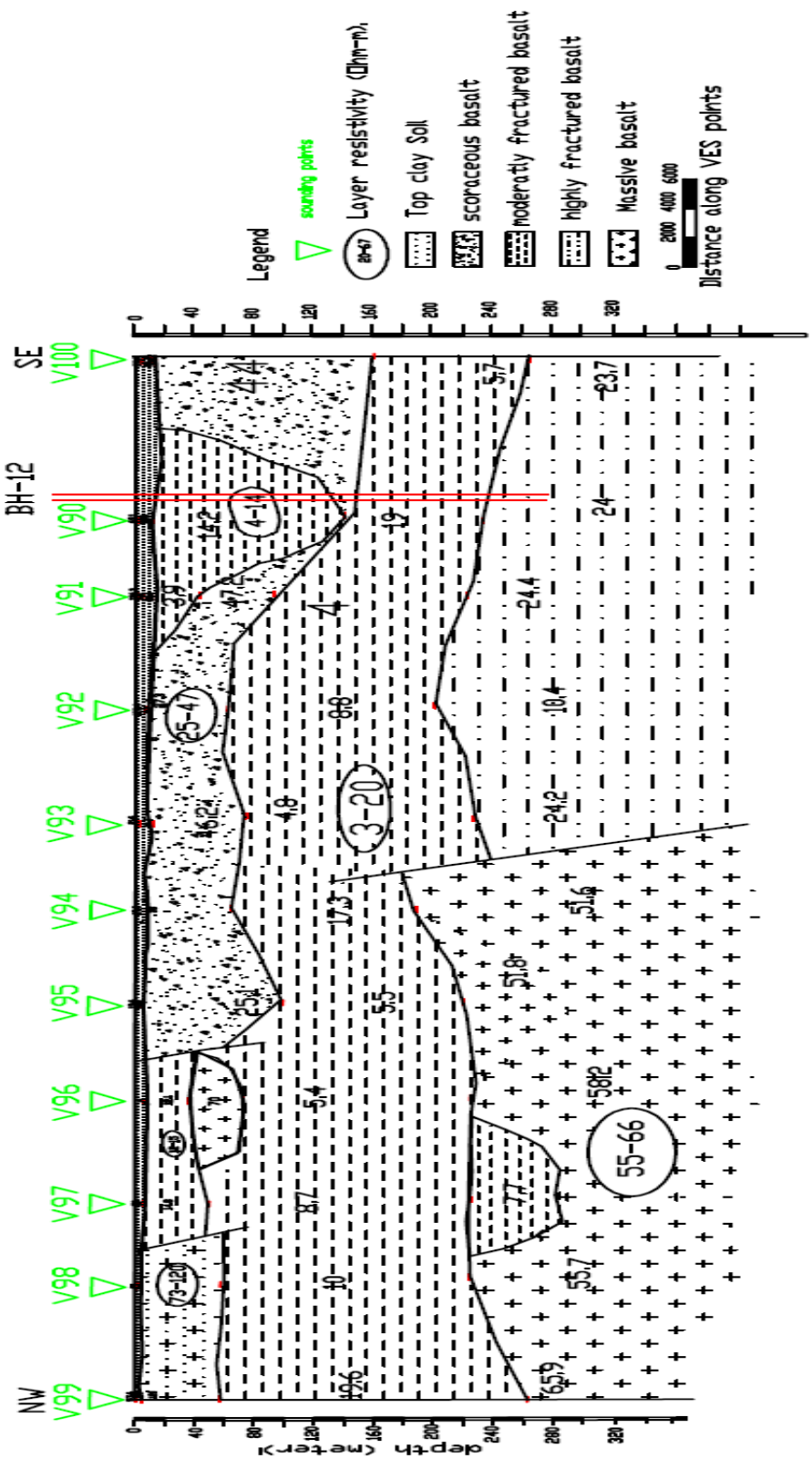

Figure 4.3 Geoelectric section along Line-1, Alidege plain.

The layer mapped as the fourth layer on the section is an extensive horizon covering the whole line with resistivity ranges between (3 to 20 Ohm-m). This Moderately to Highly weathered & fractured Basalt layer has a considerable thickness about 180 m thick that extends from an average depth of 60 m to 240 m depth. The bottom layer mapped with the survey spacing used is again a region showing relatively high resistivity (55 to 66 Ohm-m) massive basalt on the northwestern half of the line while a low resistivity (10 to 24 Ohm-m) region is mapped on the southeastern half. These lateral variations in resistivity are suggestive of the presence of a structure, possibly a fault zone somewhere between VES-93 and 94 and geologically highly fractured basalt.

From the point of view of the objective of the survey, the regions on the southeastern side of the line (i.e. between VES-94 and VES-100) are zones that a borehole sunk to depths in excess of 250 m will likely tap groundwater.

3.4.2 Traverse Line-2

This line is the survey line again on the southwestern part of the surveyed area on the Alidege plain and is oriented in north west to south east direction running almost parallel to Line-1. The line has a total length of about 21.7 km and there are 10VES (VES points 1-12) with average VES point spacing of about 2.2 km. The representative pseudodepth and geoelectric sections for the Line are presented in Figures 4.4 and 4.5 and are discussed below.

A. Pseudodepth section along Line-2

As the pseudodepth section of this profile shows (Figure 4.4), the top layer mapped around VES-1 is of relatively very high resistivity compared to the others on the line i.e. with the rest nine VES points lying on the low resistivity region. Overall, it is seen that the vast portion of the section is covered by low resistivity zone. The resistivity ranges (5 to 45 Ohm-m) of this low resistivity region are to be expected for potential water saturated area in the Ethiopian Rift.

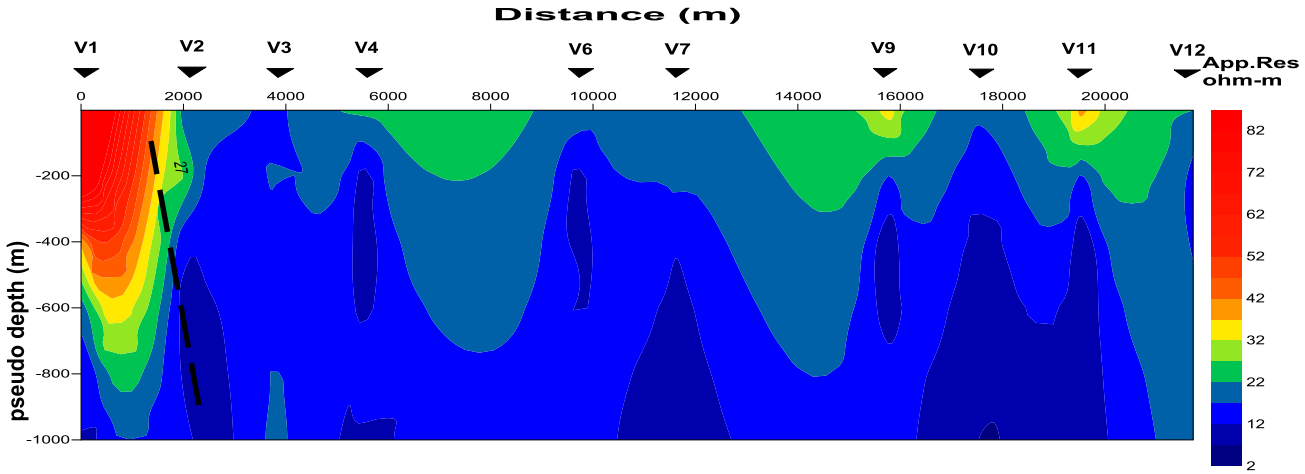

Figure 4.4 Pseudodepth sections along Line-2, Alidege plain.

B. Geoelectric section along Line-2

From the interpreted layer parameters of VES-1 to VES-12 on this line (sample interpretations of the individual VES are shown in Annex-1) the resistivity sounding geoelectric section given in Figure 4.5 is constructed. Borehole BH-2, which is located near Line-2; was also used to constrain the depth and thickness of the layers during interpretation of the sounding data and also to identify the lithological units beneath these VES points during modeling.

In quintessence the lithological description of the borehole depth section (given in Annex 2) with their resistivity parameters from each interpreted VES were used to prepare the geoelectric section.

From the section given in Figure 4.5, it is seen that the subsurface consists of 4 to 5 geoelectric horizons. The layer on the top part of the section, which is difficult to represent with the given scale, consists of two-three layers whose resistivity values show large lateral variations. The resistivity ranges between 2 Ohm-m to 520 Ohm-m well represent this portion of the section and the average thickness of this horizon is 7m.

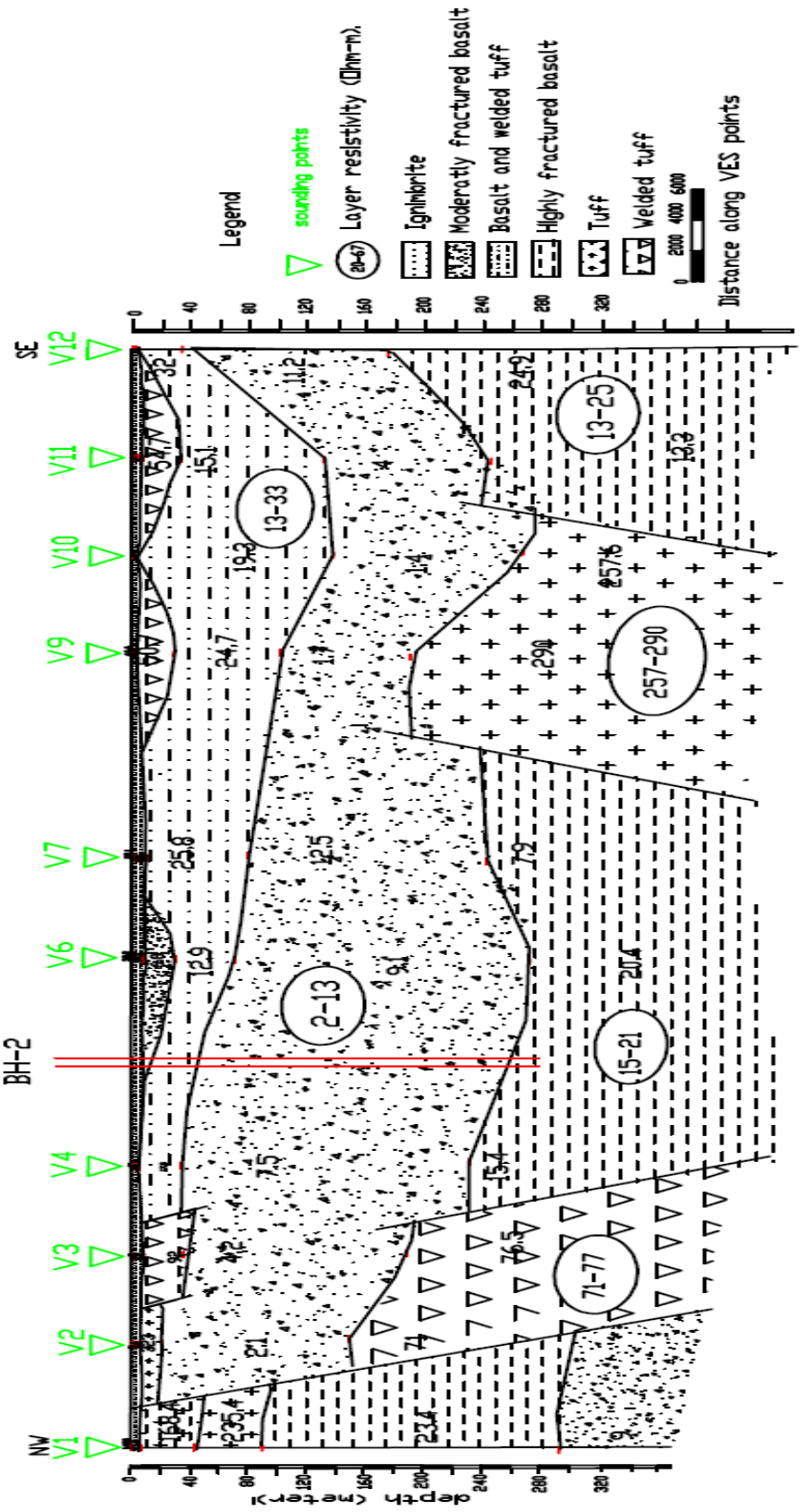

Figure 4.5 Geoelectric section along Line- 2, Alidege plain.

Beneath these layers is a relatively low resistivity horizon (13 to 33 Ohm-m) representing the moderately to highly weathered and fractured scoraceous basalt, basalt and welded tuff. This layer covers the whole section except some interruption between VES-2 and VES-4. Its thickness extends from a depth of about 8 m on the northwest side of the line to about 70 m on the average with the layer becoming thick (120 m) around VES-10 and VES-11. There are two possible minor structures and one major structure (between VES-1 and VES-2) that extend to the bottom of the layer.

The third layer on the section is an extensive horizon of low resistivity covering from the northwestern most end part of the line to southeast direction, with resistivity ranges between 2 to 13 Ohm-m. This moderately fractured basalt layer has a considerable thickness of about 200 m that extends from an average depth of 40 m to 240 m depth. The low resistivity values again suggest that the layer is potentially water bearing. The bottom layer mapped with the survey spacing used is again a region showing repeated sequence of relatively high resistivity and low resistivity horizons. But the central part of this line is the highly fractured basalt (correalable with the lithologic log of BH-2) with resistivity range between 15 Ohm-m to 21 Ohm-m. These lateral variations in resistivity are suggestive of the presence of four structures, possibly a fault zone somewhere between VES-1 and VES-2, VES-2 and VES-3, VES-7 and VES-9, and between VES-10 and VES-11.

From the objective of the study, the regions which are located in the central part of the line (i.e. between VES-4 and VES-6 are zones that a borehole sunk to depths in excess of 260m will likely tap groundwater, From these results, it is recommended that borehole (BH-2) could preferably be shifted to the southeast i.e. to the center of the traverse line to obtain a better yield from the borehole.

4.3.3 Traverse Line-3

This line is close to the center of the surveyed area on the Alidege plain and is again oriented in the northwest to south east direction and running almost parallel to Lines-1 and 2. .Nearly

regularly spaced 12 VES points lie on the profile whose length is 23.5 km; thus giving an average spacing between the VES points that is equal to 2 km.

A. Pseudodepth section along Line-3

Figure 4.6 shows the pseudodepth section constructed for the 12 VES points that lie on this survey traverse Line-3. According to this figure, there is a distinct lateral variation in resistivity, some part of the section are high resistivity zones mapped around VES-13, VES-14 VES-23 and VES-24 with resistivity rang of 32 Ohm-m to 82 Ohm-m. Or else, the vast region under the section shows wide coverage of the low resistivity zone. The resistivity ranges (2 to 22 Ohm-m) of this low resistivity region are indicative of potential water saturation, with the need to closely look into the opportunity of this low resistivity resulting from higher mineralized groundwater.

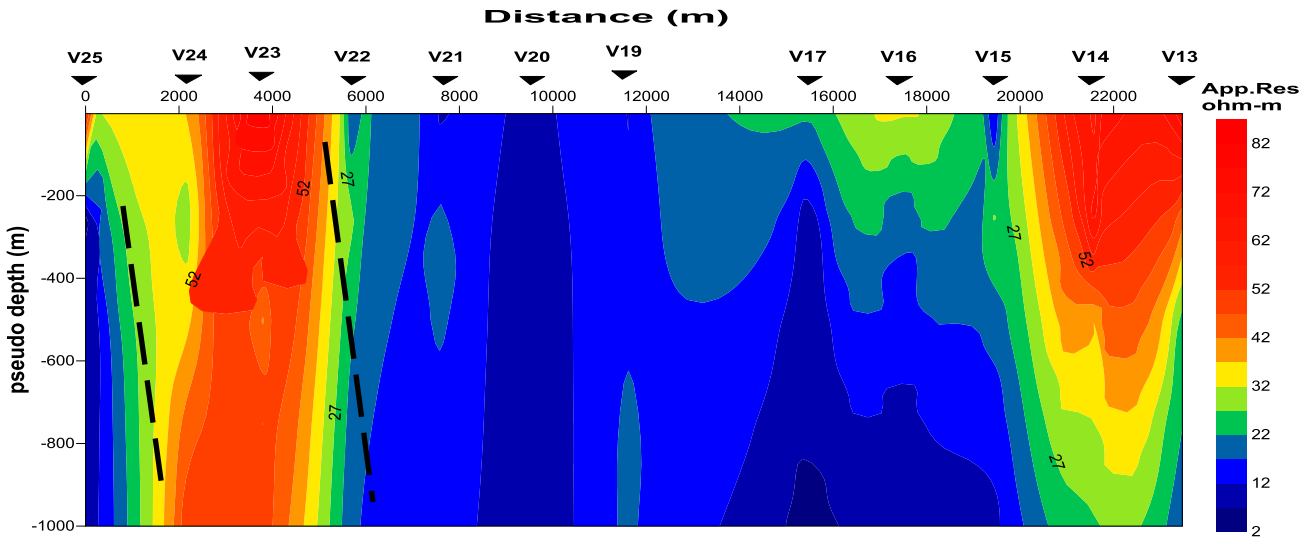

Figure 4.6 Pseudo sections along Line-3, Alidege plain.

B. Geoelectric section along Line-3

The resulting geoelectric section constructed from the interpreted layer parameters of the 12 VES (sample interpretations of the individual VES are shown in Annex-1) is shown in Figure 4.7. A

borehole BH-9 (given in Annex 2) is located near Line-1; especially close to VES-17 was also used to constrain depth and identify the lithological units beneath these VES points during modeling.

From the interpreted geoelectric section along Line-3, subsurface consists of 5-6 geoelectric horizon.
The layer representing the top part of the section, which is complicated to represent with the given scale, consists of two-three layers whose resistivity values show large lateral variations. These variations are believed to result from either difference in lithology or soil humidity content. Beneath these layers a relatively low resistivity (2 to 6 Ohm-m) moderately weathered & fractured ignimbrite horizon is covering the region from northwest direction towards south east direction. Its thickness extends from a depth of about 8m to about 30m on the average.

But towards northwest there are two structures between VES-23 and VES-24 and between VES-24 and VES-25 respectively, the region intersected by these structures has relatively low 1.6 Ohm-m and relatively high resistivity zone 21.3 Ohm-m and its thickness extends from a depth of about 8m to about 40 m on the average.

The third layer on the section starting from northwest most end of the line has low resistance horizon (5 to 39 Ohm-m), towards the center of the line relatively very high resistive horizon (141 to 268 Ohm-m) geologically represented as weathered basalt, at the central part of the line relatively very low resistive horizon (10 to 20 Ohm-m); its thickness about 70m and from the central part of the line towards the southeastern most end of the line high resistive horizon (74 to 140 Ohm-m). This layer categorize by four structure, the first structure occurs between VES-24 and VES-25, between VES-23 and VES-24, between VES-19 and VES-20 and between VES-24 and VES-25 respectively.

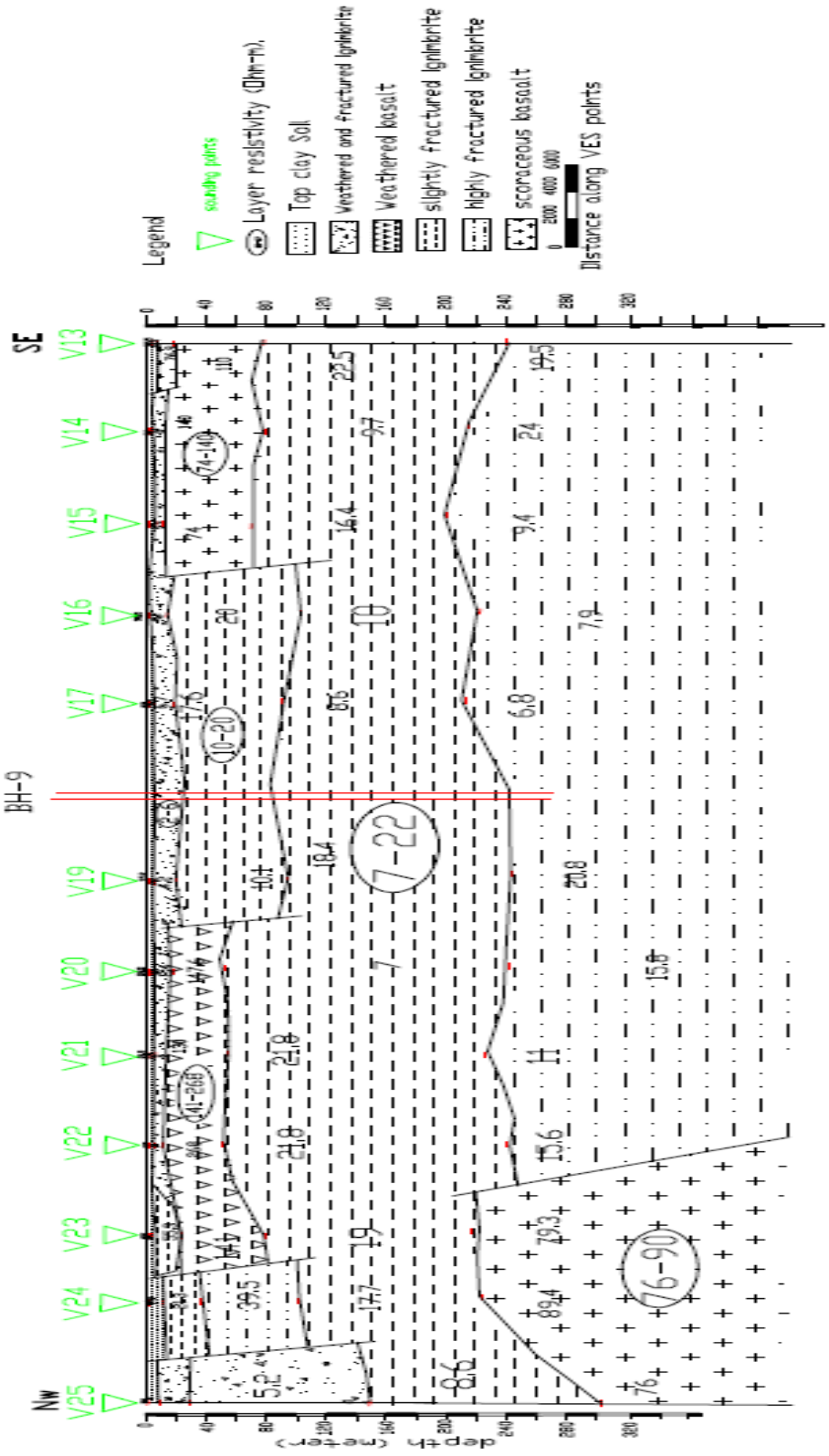

Figure 4.7 Geoelectric section along Line-3, Alidege plain.

The layer mapped as the fourth layer on the section is slightly to moderately fractured basalt, scoraceous basalt and moderately ignimbrite .It is an extensive horizon covering the whole line with resistivity ranges between (7 to 22 Ohm-m). The layer has a considerable thickness about 150 m thick that extends from an average depth of 100 m to 250m depth. The bottom layer mapped in this profile has slightly fractured scoraceous basalt, from northwest towards near to the center of the line relatively high (70 to 90 Ohm-m) horizon while highly fractured ignimbrite towards the southeast direction relatively low resistivity horizon. There is one structure between VES-22 and VES-23, possibly fault. The low uniform resistivity of the layer may indicate the resemblance in water bearing capacity and yield of aquifer under the fourth layer.

4.3.4 Traverse Line-4

This traverse line is the center on the Alidege plain and is again oriented in North West to south east direction and running almost parallel to Lines-1,2 and 3 The line has a total length of about 24 km and there are 11 VES (VES points 26-38 with average VES point spacing of about 2.2 km.

A. Pseudodepth section along Line-4

The pseudodepth section of traverse Line-4 has constructed for 11 VES are given in Figure 4.8.From the profile, some part of the section with high resistivity top zones mapped around VES-30, VES-31, VES-34, VES-35, VES-37 and VES-38.This high resistivity zone is extend to the bottom of the section only in the region around VES-34 VES-35, VES-37and VES-38. But the other portion of region over section shows widespread coverage of low resistivity horizon (2 to 22 Ohm-m). This low resistivity region are investigative for ground water potential.

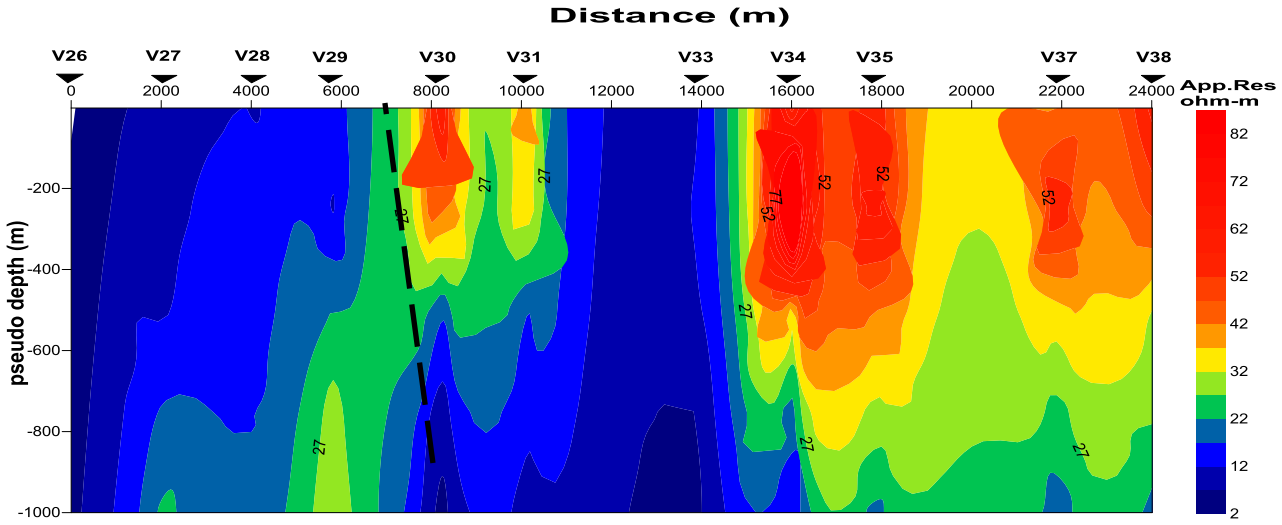

Figure 4.8 Pseudo sections along Line-4, Alidege plain.

B. Geoelectric section along Line-4

From the interpreted layer parameters of VES-26 to VES-38 (sample interpretations of the individual VES are shown in Annex-1) the resistivity sounding geoelectric section (Figure 4.9) along Line-4 is constructed. A borehole BH-4 (given in Annex 2) is located near Line-4; in particular close to VES-31 was also used to confine depth and identify the lithological units beneath these VES points during modeling.

From the above Figure, the subsurface consists of 5 geoelectric horizons. The layer representing the top part of the section, which is difficult to represent with the given scale, consists of one-two layers whose resistivity values show large lateral variations. Beneath these layers there is intercalation of relatively low, high and very high and its thickness extends from a depth of about 10 m to about 40m on the average. In this substratum their is one major structure lies to near the center of the traverse line that extends to the bottom of the layer between VES-29 and VES-30 and there are minor structure in this horizon.

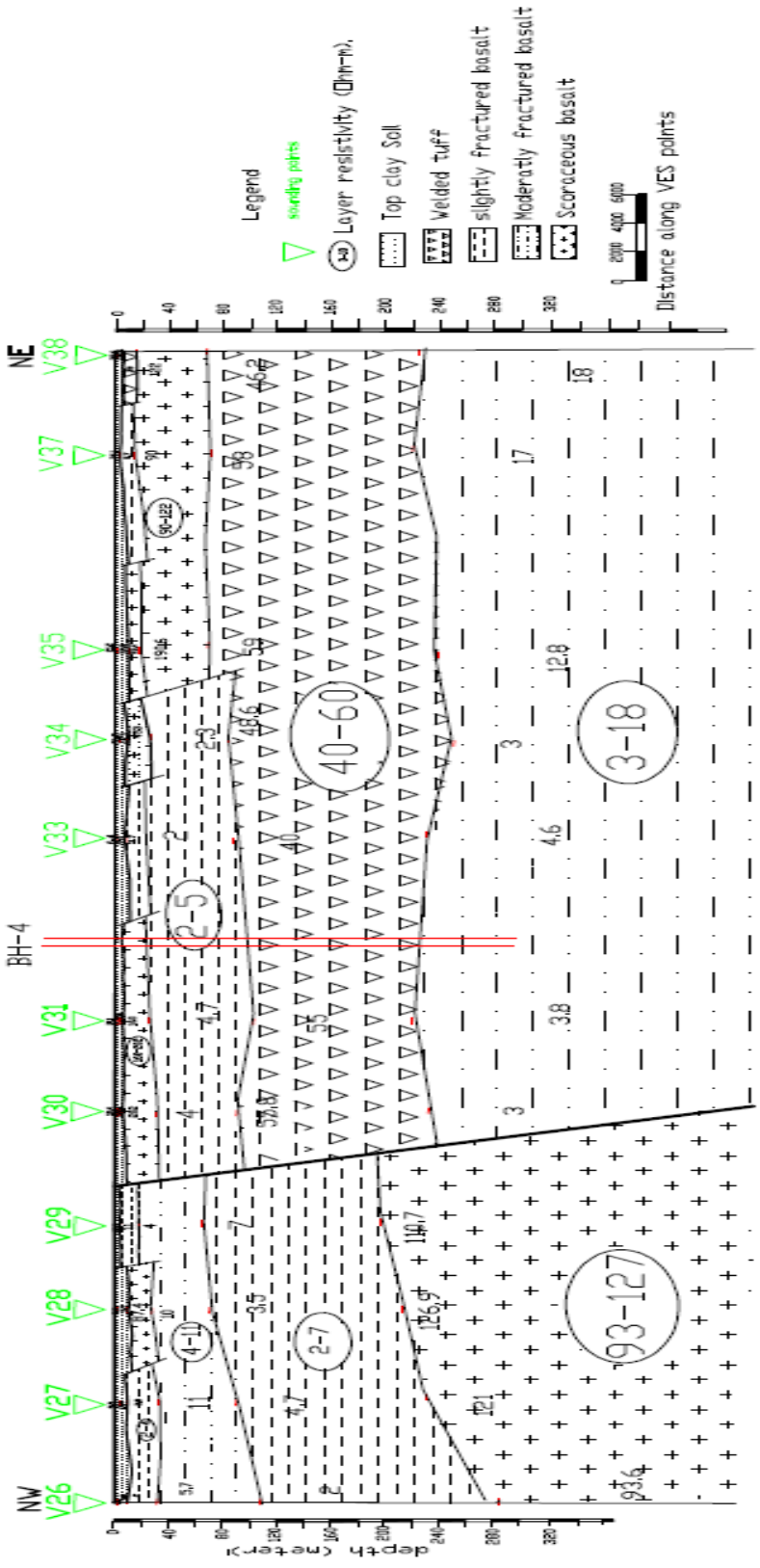

Figure 4.9 Geoelectricsection along Line -4, Alidege plain.

The third layer has moderately fractured basalt with resistivity of 4 to 11Ohm-m horizon covering the region from NE direction to the major structure, a relatively low resistivity horizon (2 to 5 Ohm-m) at the center of the line about 80m thickness presented as slightly fractured basalt and towards SE direction relatively very high resistivity slightly fractured scoraceous basalt (90 to 122 Ohm-m) horizon, its thickness about 100m.

.The layer mapped as the fourth layer on the section is a region showing a relatively low resistivity (2 to 7 Ohm-m) on the northwestern half of the line while a high resistivity (40 to 60 Ohm-m) region is mapped as Welded tuff on the southeastern half. The fifth or the bottom substratum layer is marked by relatively very high resistivity ranges between (93 to 127 Ohm-m) from northwest towards the center of the line and low resistivity ranges between (3 to 18 Ohm-m) towards southeast direction, Geologically interpreted as moderately fractured basalt. This layer is most likely water –bearing horizon along the traverse.

4.3.5 Traverse Line-5

This line is lie on the northeastern most end of the Alidege plain and is again oriented in North West to south east direction and almost parallel to the other four traverse lines. The line has a total length of about 23.8 km and there are 12 VES (VES points 39-51) with average VES point spacing of about 2 km.

A. Pseudodepth section along Line-5

The pseudodepth section constructed for 11 VES that lie on traverse Line-4 are given in Figure 4.10.According to this figure, most part of the section with high resistivity top zones mapped around VES-43, VES-44, VES-48, VES-49, VES-50, VES-51, and VES-85.These high resistivity zone is found to some extend to depth of the section only the region around VES-44 and VES-85. Although the vast area under the section shows extensive coverage of low resistivity horizon (4 to 25 Ohm-m).

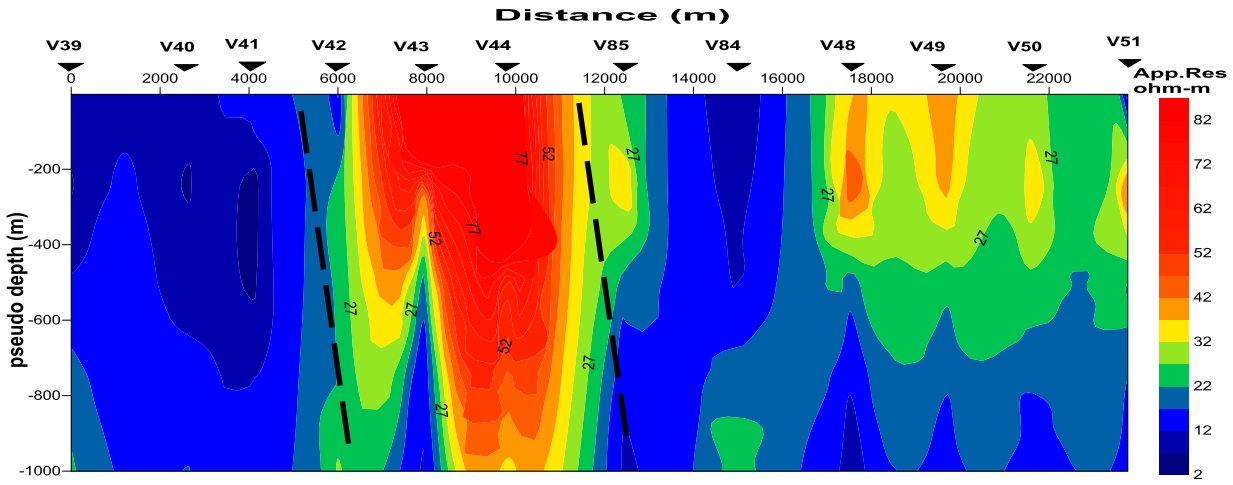

Figure 4.10 Pseudo sections along Line-5, Alidege plain.

B. Geoelectric section along Line-5

Along this traverse line there are 11 VES points; the geoelectric section is constructed from the interpreted layer parameters of VES-39 to VES-51 (sample interpretations of the individual VES are shown in Annex-1) is shown in Figure 4.11. Borehole BH-3 is located around Line-5 was also used to confine depth and identify the lithological units beneath these VES points during modeling. In essence the lithological description of the borehole depth section (given in Annex 2) with their resistivity parameters from each interpreted VES were used to prepare the geoelectric section. From the figure 4.11, the subsurface consists of 5-6 geoelectric horizons.

The upper most layer is difficult to correspond to with the given scale, consists of two-three layers whose resistivity values show large lateral variations. The second layer a relatively very low resistivity horizon (4 Ohm-m) covering by highly weathered & fractured basalt the region at the center of the line and low resistivity horizon (11 to 24 Ohm-m) towards NW direction, elsewhere relatively very high (300 to 406 Ohm-m) ignimbrite lithology description observed from borehole-3.

Beneath this layer very high resistivity horizon (100 to 350 Ohm-m) at the center of the line and its thickness extends from a depth of about 30 m to about 80 m on the average and this ignimbrite layer becoming thick (100 m) around VES-43 and VES-44 ,towards NW direction relatively very

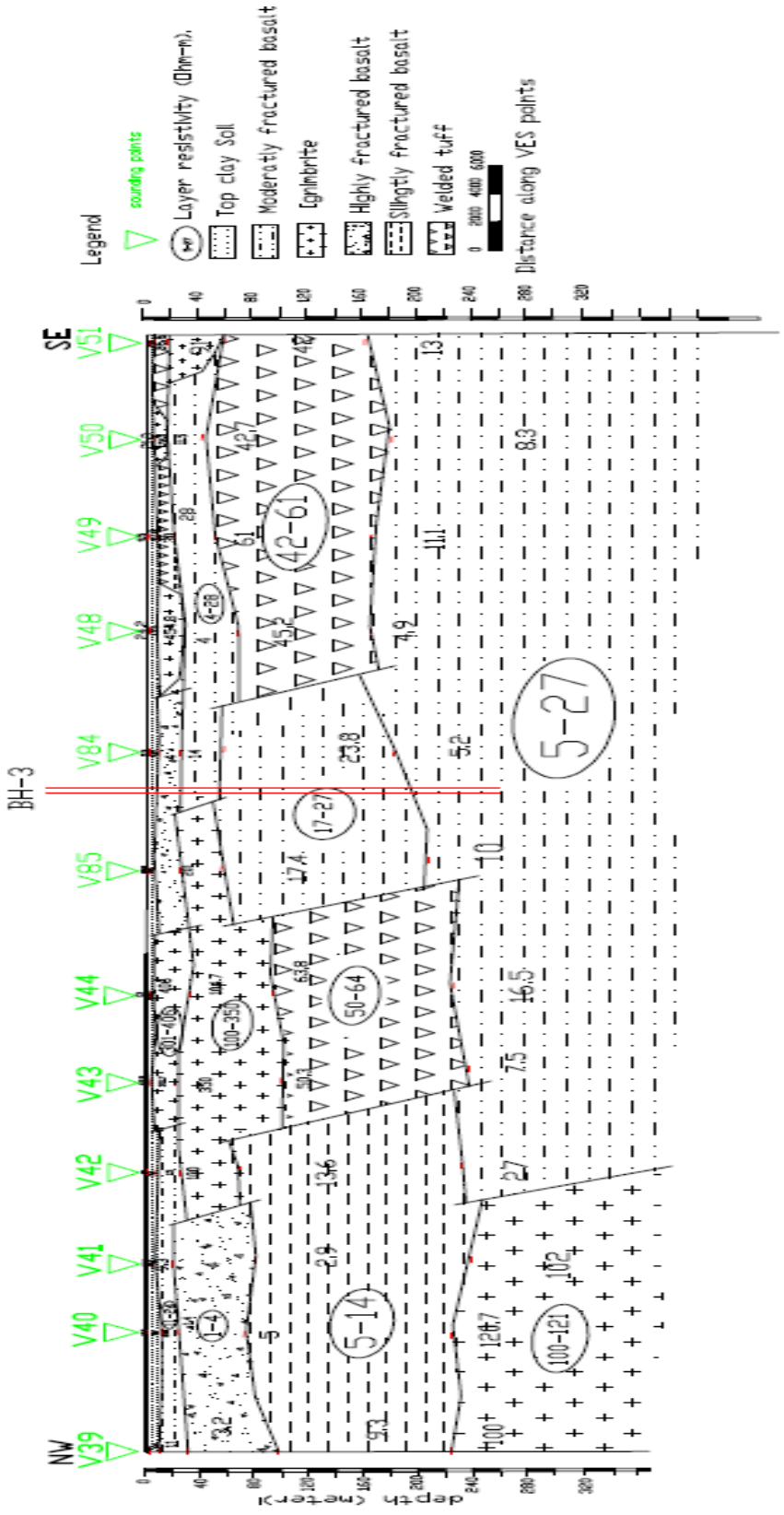

Figure 4.11Geoelectric section along Line 5, Alidege plain.

low resistivity horizon (1 to 4 Ohm-m) and the region from the center of the line towards SE direction e moderately fractured basalt with resistivity range of (4 to 28 Ohm-m) horizon ,its thickness extends from a depth of about 20 m to about 60 m on the average.

The fourth layer has moderately fractured basalt with relatively low resistivity range (17 to 27 Ohm-m) at the center of the line. The thickness extends from a depth of about 80 m to about 210m (130 m thick) on the average. The low resistivity response of this layer shows that it is possibly water saturate, towards SE direction relatively high resistivity (42 to 61 Ohm-m) Bluish welded tuff, towards NW direction relatively low resistivity (5 to 14 Ohm-m) and its thickness extends from a depth of about 100m to about 220m.the layer could be subdivided by three structure from NW towards SE direction the first structure may be fault lie the region between VES-42 and VES-43,the second structure lie on the region between VES-44 and VES-85 and the third structure lie between VES-48 and VES-85.

The bottom layer mapped with the survey spacing used is again a region showing a relatively high resistivity (100 to 121Ohm-m) ignimbrite lithology on the northwestern somewhat near to half of the line while a low resistivity (10 to 24 Ohm-m) region is mapped on the southeastern half. These lateral variations in resistivity are indicative of the presence of a structure, possibly a fault zone somewhere between VES-41and 42. From the point of view of the objective of the assessment, the regions on the central part of the line (i.e. between VES-84 and VES-85) are zones that a borehole sunk to depths in excess of 250 m will likely tap groundwater.

4.3.6 Traverse Line-6

This line is the survey line again on the cross part of the surveyed area on the Alidege plain and is oriented in north east towards south west direction running almost perpendicular to those five parallel lines. The line has a total length of about 47 km and there are 11 VES (VES points 55-1) with average VES point spacing of about 4.2 km.

.

A. Pseudodepth section along Line-6

The pseudodepth section constructed for the 11 VES that lie on the survey traverse Line-6 are given in Figure 4.12. From the figure below, very high resistivities zone is found from the top of the region to the bottom of the region mapped around VES-55, VES-73 and partially VES-71 with the rang (213 to 363 Ohm-m) .The upper most portion of VES-1 and VES-5 show high resistivity zone, elsewhere he vast region under the section shows extensive coverage of the low resistivity zone (3 to 83 Ohm-m). The resistivity ranges of this low resistivity region are indicative of potential water saturation.

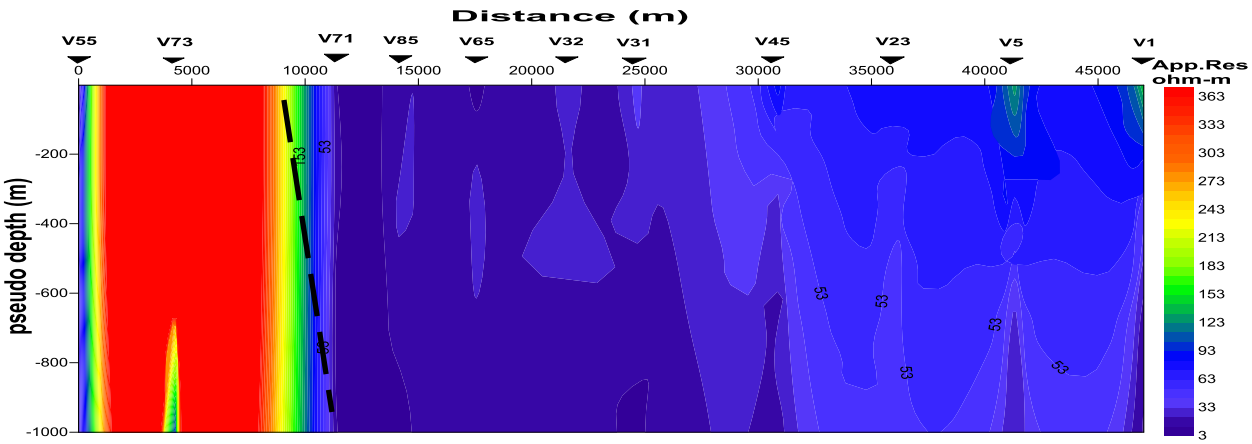

Figure 4.12 Pseudo sections along Line-6, Alidege plain.

B. Geoelectric section along Line-6

The resulting geoelectric section constructed from the interpreted layer parameters of the 11VES i.e. from VES-55 to VES-1 lying on this traverse is given in Figure 4.13.Borehole BH-4 is located near Line-6; especially close to VES-31 was also used to constrain depth and identify the lithological units beneath these VES points during modeling. In real meaning, the lithological description of the borehole depth section (given in Annex 2) with their resistivity parameters from each interpreted VES were used to prepare the geoelectric section shown below (Figure 4.13).

From the geoelectric section, the sub surface consists of 5-6 geoelectric horizons. The topmost layer is a thin layer; its thickness varies from 0.4m to 18.3m, which is difficult to represent with

the given scale, consists of two-three stratums whose resistivity values show large lateral variations.

Here the variation in resistivity values of top layer could result from the variation in moisture (water) content contained in the top soil of the wet marshy ground. Beneath these layers has slightly fractured scoraceous basalt a relatively very high resistivity extensive horizon covering the whole line with resistivity ranges between (100 to 350 Ohm-m) and Its thickness extends from a depth of about 20 m to about 60 m on average with the layer becoming thick (90m) around VES-55.

The third layer has low resistivity horizon (3 to 19 Ohm-m) geologically expressed as moderately fractured basalt, covering the region from the northwestern part of the line towards southeaster direction, but not able to southeaster end; untile to the structure and its thickness extend from the depth of about 90m to about 140 m on average, but the layer becoming thin (100) around VES-23.

The structure may be fault found between VES-5 and VES-23. The region from this fault to southeastern end of the line occupied by very high resistivity horizon with the range (235 to 383 Ohm-m) and 50 thick.

The forth layer of this section has welded tuff at the central part of the line, covered by relatively moderate resistivity horizon (42 to 68 Ohm-m) and its thickness extends from a depth of about 140m to about 260m, a relatively low resistivity horizon (4 to 24 Ohm-m) represented as slightly fractured basalt covering the region from the center of the line towards NW direction. Its thickness extends from a depth of about 150 m to about 260 m on the average with the layer becoming thick (280m) around VES-65 and VES-85.The region from the center of the line towards SE direction is covered by low resistivity horizon (20 to 24 Ohm-m). Its thickness extends from a depth of about 100 m to about 240 m on the average.

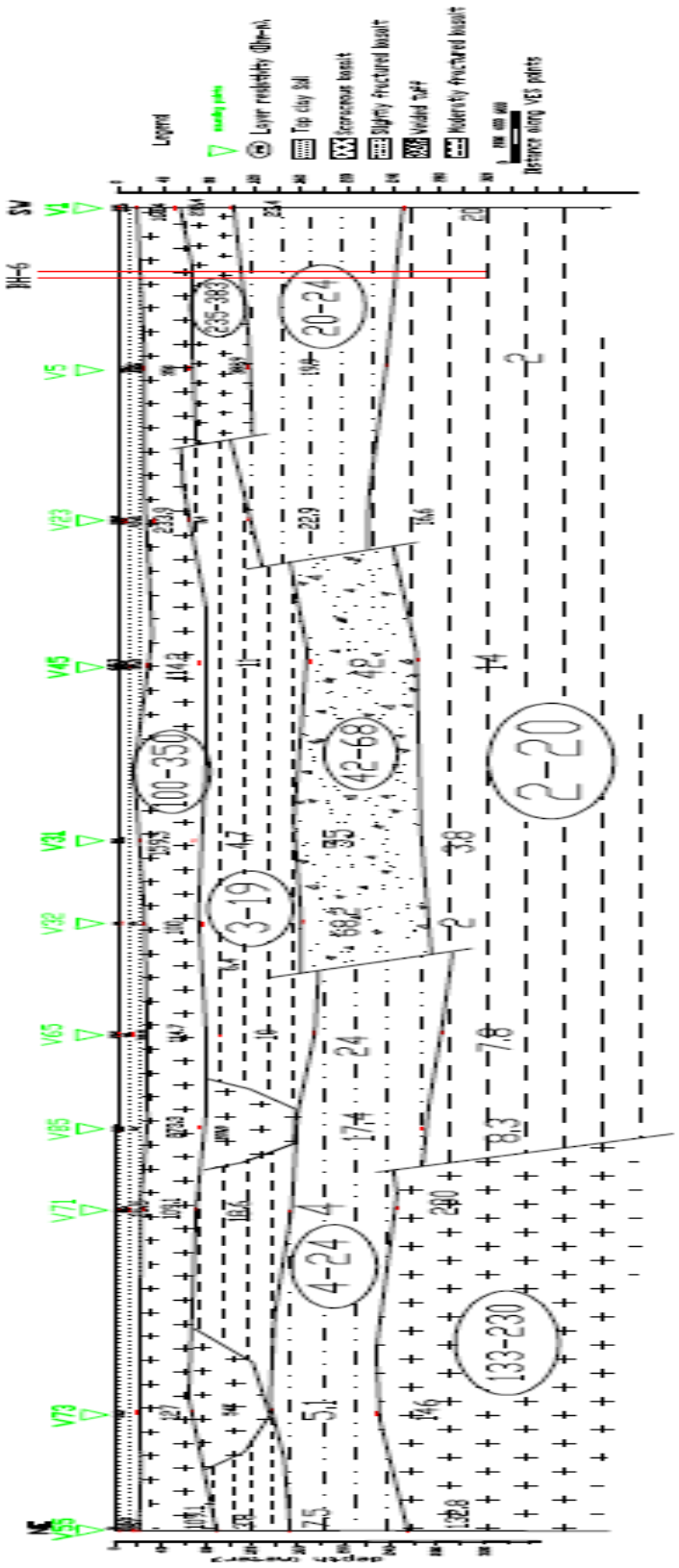

Figure 4.13 Geoelectric section along Line 6, Alidege plain.

The bottom layer mapped as high resistivity horizon (133 to 230 Ohm-m) from NW side of the line near to the center part of the line and from the northwest half of the line towards SE direction is covered by moderately fractured basalt with low resistivity range of 2 to 20 Ohm-m. This low resistivity ranges preferably be water bearing horizon. There is one structure, may be fault somewhere between VES-71 VES-85.

From the point of view of the objective of the survey, it is recommend that BH-6 expected to be sunk the regions on the southeastern side of the line (i.e. between VES-1and VES-5) to the depths in excess of 250 m will likely tap groundwater.

CHAPTER FIVE
CONCLUSION AND RECOMMENDATION

5.1 Conclusions

This work presented the results of geophysical survey that was conducted in the Alidege plain of Afar Regional State, northeastern Ethiopia. The Alidege plain is a vast, flat rolling plain with a total area of about 1650 sq km located at the opening of the Main Ethiopian Rift towards the Afar. The aim of the work is to investigate the general groundwater potential of the area, map areas of groundwater saturation, map possible structures that could control the movement of fluids and from these studies suggest likely areas for sinking of productive boreholes. For the study, a total of 90 VES conduced by the Water Works Design and Supervision Enterprise (WWDSE) as a national project to study the groundwater potential and implement the resource for irrigation works and grazing land development for the pastoral population of the area.

The VES were carried out with the OYO MCOHM Mark-2 resistivity meter with optimal half current electrode (AB/2) spacing of 1000m. The 90 VES were distributed over the study area at an average spacing of a VES point for every 18 sq km, a distribution adequate for regional study.

The interpretations of all the VES were made qualitatively as well as quantitatively to achieve the desired objectives. The qualitative interpretation of the VES data was performed by preparing a sliced-stacked apparent resistivity maps and pseudodepth section maps for six selected traverse lines. The quantitative interpretation of the VES data were made through direct interpretation of the inversion of the individual VES using a combination of software and preparing geoelectric sections along five parallel and one cross profiles. Additional inputs from a number of test boreholes that were drilled over the area to validate and confirm the results of a number of VES carried out during the initial phase of the project were also incorporated and used to constrain the VES interpretation. The uses of the borehole lithologic logs have strongly facilitated the interpretation of the geoelectric sections in terms of different lithologic units.

Based on the result discussion and interpretation, the following conclusions have been drawn using the combination of data presentation approaches:

1. The apparent resistivity pseudodepth sections and the true resistivity geoelectric sections show the presence of shallow as well as deeper low resistivity horizons which are potential zones of groundwater saturation. The low resistivity and large thickness of these horizons is an indicator of high groundwater potential in the study area.

2. From the result of the electrical resistivity surveys, it is also seen that the area is highly affected by tectonic forces that have resulted in major fracturing and faulting of the rock units at varying depths. These faults and fractures are believed to control the flow of groundwater. The fractures and weak zones are the major controls for the flow of ground water over the area. Most of basaltic rocks (for traverse Lines-1, 2, 4,5 and traverse Line-6) and ignimbrites (for traverse Line-3) are highly fractured and expected to be the water-bearing zones at different depths.

3. The geological structures (fractures, faults and contacts) play a great role in the movement and occurrence of the groundwater in the study area. The highly to moderately weathered and fractured ignimbrites and basalts contribute more for the recharge and movement of the groundwater through the faults and wake zones.

4. Comparison of the geophysical interpretations with drilled borehole results show that the results of geophysical survey are good correlation with the borehole logging results.

5. The main geologic units encountered over the survey area that are likely to bear groundwater (based on the degree of fracturing and weathering) are basalts, ignimbrites, rhyolites and welded tuff.

6. Some of the important locations and depths to water bearing horizons over the survey traverse lines are as follows:

- Traverse Line-1: As shown in Figure 4.3, the water-bearing horizon is mapped to be at the depth between 250m to 300m.
- Traverse Line-2: A borehole (BH-2) preferably drilled to a depth of range between 240m to 280m and between VES-4 and VES-6 may yield high volume of groundwater (Figure 4.5)
- Traverse Line-3: From Figure 4.7, the depth of the water-bearing horizon is at the depth 250m.
- Traverse Line-4: As shown in the Figure 4.9, at the depth between 240m to 260m has the water-bearing horizon.
- Traverse Line-5: A borehole (BH-3) expected to be sunk at the depth of range between 160m to 240m and around between VES-84 and VES-85 may give high amount of water (Figure 4.11)
- Traverse Line-6: A borehole (BH-6) expected to be sunk at the depth range between 260m to 300m and around between VES-1 and VES-5 may give higher volume of groundwater. (Figure 4.13).

These have been indicated as preferred locations for the sinking of boreholes to extract good amount of groundwater. A drilling program- both test and productive- is suggested to focus on these areas.

5.2 Recommendations

Based on the outcomes of this study, the following recommendations are forwarded:

1. According to the interpretation of the VES, geoelectric section along traverse Line-2 shows that if BH-2 could preferably be shifted to the near central part of the line between VES-4 and VES-6 the likelihood of extraction of higher volume of groundwater is increased.
2. As seen have seen on result and interpretation part, borehole (BH-3) preferably to sunk on the traverse Line-5 between VES-84 and VES-85.
3. From the geoelectric section along traverse Line-6, borehole (BH-6) should be sunk on the southeastern part of the line between VES-1 and VES-5.
4. Other test boreholes (BH-12, BH-9 and BH-4) are expected to put as it is, but it should be increase the depth to obtain better yield of the boreholes.
5. In order to map the network of fractures and faults and validate the results of this work in respect to mapping of subsurface weak zones in better detail additional geophysical methods- for example like resistivity imaging surveys and magnetic surveys- must be employed only in selected areas.

REFERENCES

Bilham, R., Bendick, R., Larson, K., Mohr, P., Braun, J., Tesfaye, S., and Asfaw, L., 1999; Secular and tidal strain across the Main Ethiopian Rift; Geophysical Research Letters, **26**, 278–2792.

Boccaletti, M., Mazzuoli, R., Bonini, M., Trua, T., and Abebe, B., 1999; Plio–Quaternary volcanotectonic activity in the northern sector of the Main Ethiopian Rift; Relationships with oblique rifting. Journal of African Earth Sciences, **29**, 679–698.

Curry, D.T., May 1972; Geomorphic, geological and groundwater studies in the Awash Valley; Informal Technical Report No. 4. UNDP/SF/ETH. 25.

Curry, D.T., April 1974; Earth Resources Technology Satellite I use, and additional ground water studies in the Awash valley; Informal Technical Report No. 4. UNDP/FAO/ETH 72/006.

Chernet, T., Hart, W.K., Arnson, J.L. Walter, R.C., 1998; New age constraints on the timing of volcanism and tectonism in the northern Main Ethiopian Rift – Afar transitional zone; Journal of Volcano logy and geothermal research, 80, 267 – 280.

Dobrin, M.B. and Savit, C. H., 1988; Introduction to geophysical prospecting, fourth edition. McGraw-Hill, New York, USA .Pp498-613,750-837.

Fetter, C.W., 2001; Applied Hydrogeology,4th Edition. Prentice-Hall, Inc.

Gibson, P.J.and George, D.M., 2003; Environmental applications of geophysical surveying techniques. Nova Science Publishers, Inc. New York.

Giday WoldeGabriel, G., Aronson, J., and Walter, R., 1990; Geology, geochronology, and rift basin development in the central sector of the Main Ethiopian Rift. Geological Society of America Bulletin, 102, 439–458.

Geo Engineering Service, 2003; Hydrogeological studies at eight sites in Boke and Meiso Woredas of West Hararge Zone, Afar, Ethiopia.

Golden software, 2010; surfer, version 9.11:Inc.

Halcrow, 1989; Master plan for the development of surface water resources in the Awash basin, Vol. 7, Annex F, soils and land resources. Addis Ababa, Ethiopia.

Ketema Tadesse and Heroic Ferdinand, **1983**; Groundwater Resources of the Alaidege Plain, WWDSE, Addis Ababa, Ethiopia.

Kazmin, V., Berhe, S.M,**1972** ; Geology and development of Nazreth area, Northern Ethiopia. ; Ethiopian Institute of Geological Surveys. Note No 11.

Kazmin V., 1972; Geological map of Ethiopia, 1:2,000,000scale. Geological Survey of Ethiopia. **Makris, J., and Ginzburg, A., 1987; The Afar Depression: Transition between continental rifting and sea floor spreading**. Tectonophysics, 141, 199–214.

Mohr, P., 1967a.; The Ethiopian Rift System. Bulletin of the Geophysical Observatory, Haile Selassie I University, **11**, 1–65.

Menzies, M., Baker, J., Bosence, D., Dart, C., Davison, I., Hurford, A., Al'Kadasi, M., McClay, K., Nichols, G., Al'Subbary, A., and Yelland, A., 1992;The timing of magmatism, uplift and crustal extension: Preliminary observation from Yemen, *in* Storey, B.C., Alabaster, T., and Pankhurst, R.J., eds, Magmatism and the causes of continental break-up. Geological Society of America Special Paper, 68, 293–304.

Schilling, J. -G., **Nd-Sr-Pb (1992)**; isotopic variations along the Gulf of Aden: Evidence for Afar mantle plume–continental lithosphere interaction. Journal of Geophysical Research, 97, 10,927–10,966.

Shakeel Ahmed, Jerome Perrinand Benoit Dewandel (2006); International Conference on Water Resources and Arid Environments; Arab Water Forum.

Tesfaye, S., David J. Harding and Timothy M. Kusky, September 2003; Early continental breakup boundary and migration of the Afar triple junction, Ethiopia; Geological Society of America Bulletin, **115**, no. 9.

Telford, W.M., Geldart, L.P. and Sheriff, R.E., 1990; Applied Geophysics, 2nd Edition; Cambridge University Press, Cambridge, UK. Pp 6-48,522-562.

Vander Velpen B.P.A, 1995; RESIXIP and Winresist software, 1st version; Interpex limited.

WWDSE, 2004 ; Well Completion report on wells drilled in Awash Arba and Awash Sebat Kilo, Addis Ababa, Ethiopia Pp1-50.

Wikipedia, 2011; Geoid.Answers.com.Wikipedia.

ANNEX -1

Interpreted VES Curves

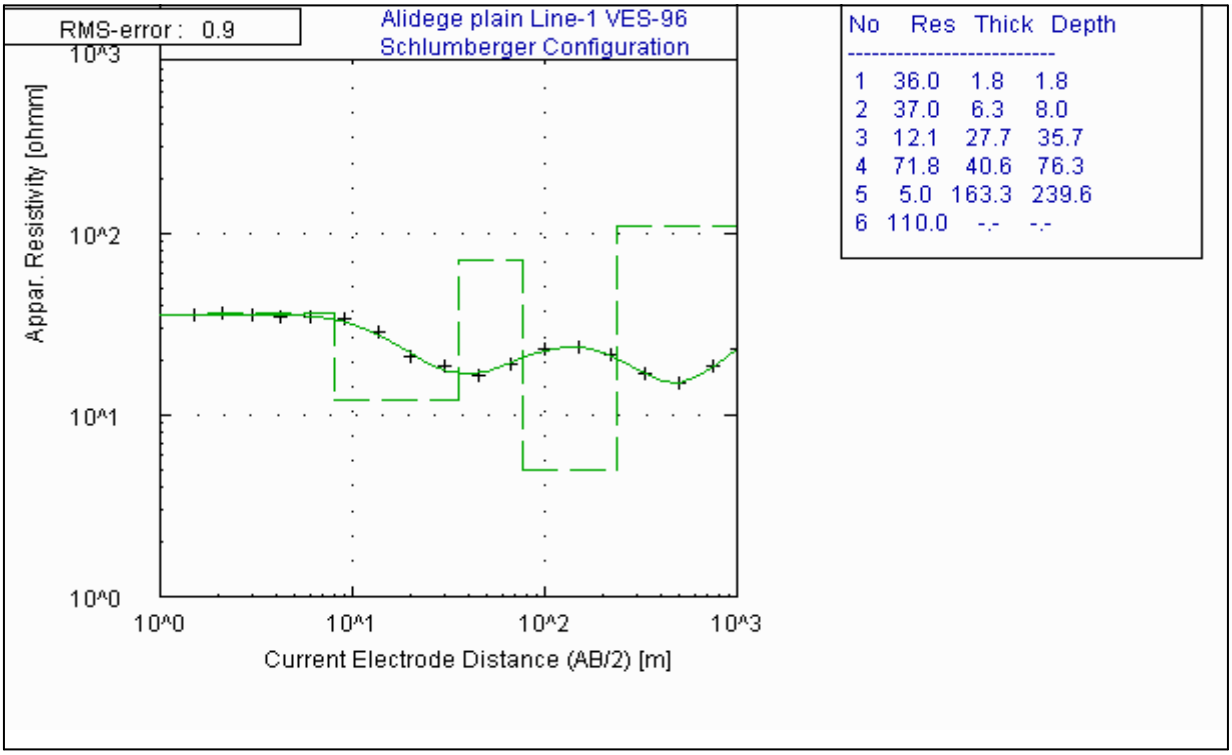

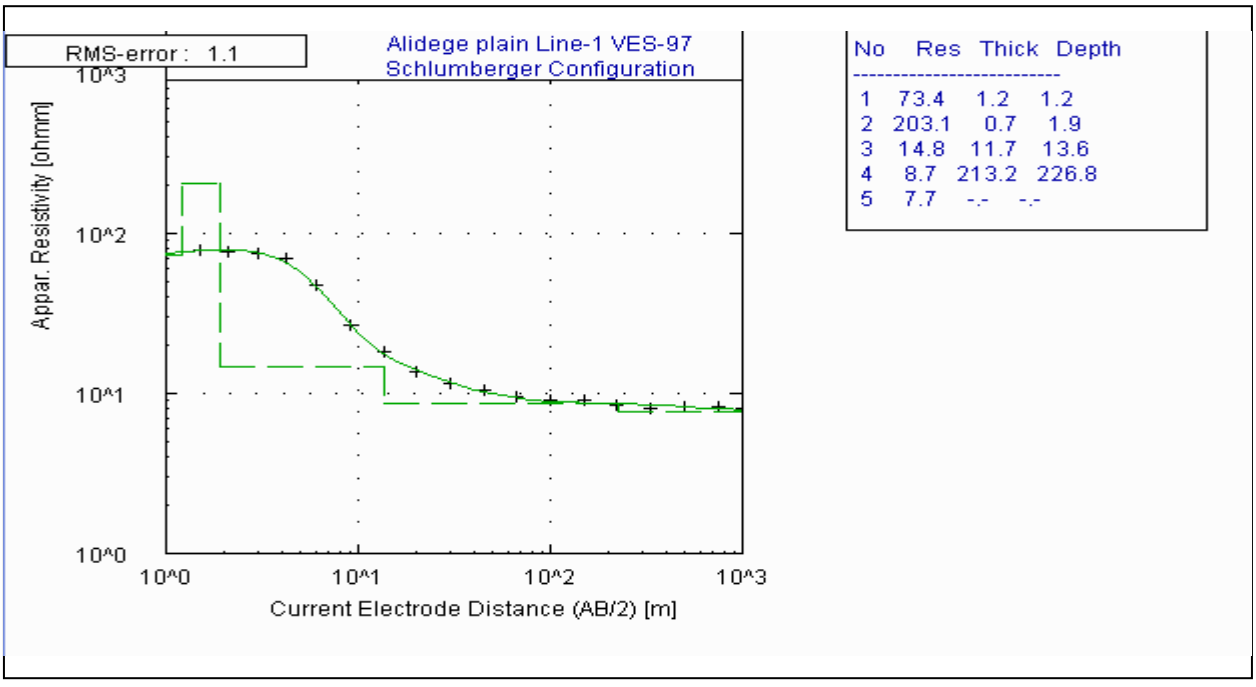

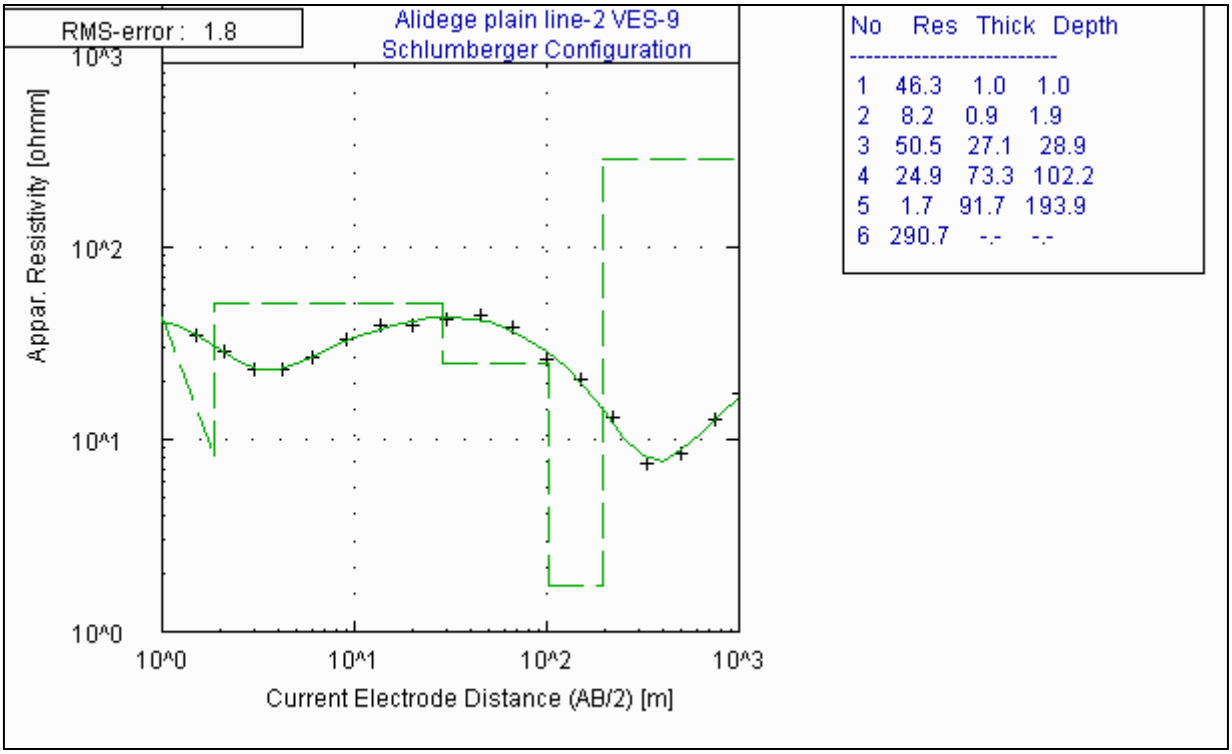
RMS-error : 1.8
Alidege plain line-2 VES-9
Schlumberger Configuration
Appar. Resistivity [ohmm]
10^3
10^2
10^1
10^0
10^0
10^1
10^2
10^3
Current Electrode Distance (AB/2) [m]
No Res Thick Depth
1 46.3 1.0 1.0
2 8.2 0.9 1.9
3 50.5 27.1 28.9
4 24.9 73.3 102.2
5 1.7 91.7 193.9
6 290.7 -.- -.-

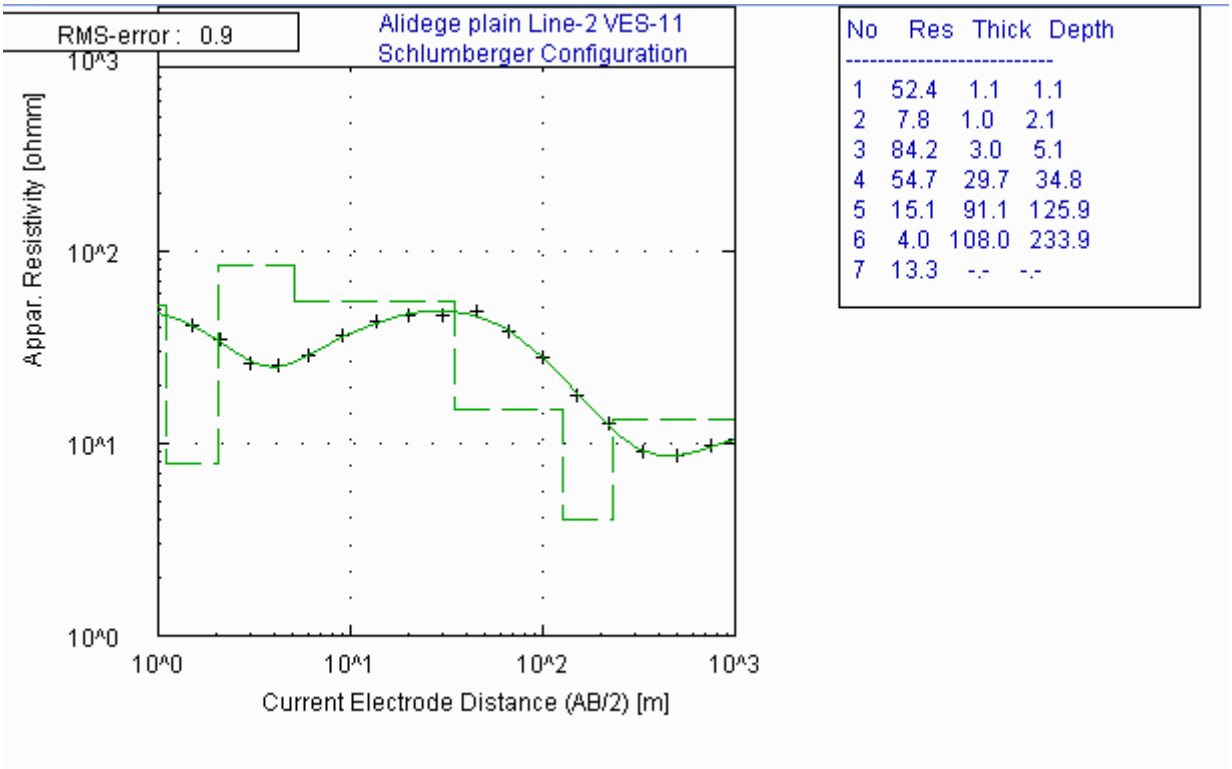
RMS-error : 0.9
Alidege plain Line-2 VES-11
Schlumberger Configuration
Appar. Resistivity [ohmm]
10^3
10^2
10^1
10^0
10^0
10^1
10^2
10^3
Current Electrode Distance (AB/2) [m]
No Res Thick Depth
1 52.4 1.1 1.1
2 7.8 1.0 2.1
3 84.2 3.0 5.1
4 54.7 29.7 34.8
5 15.1 91.1 125.9
6 4.0 108.0 233.9
7 13.3 -.- -.-

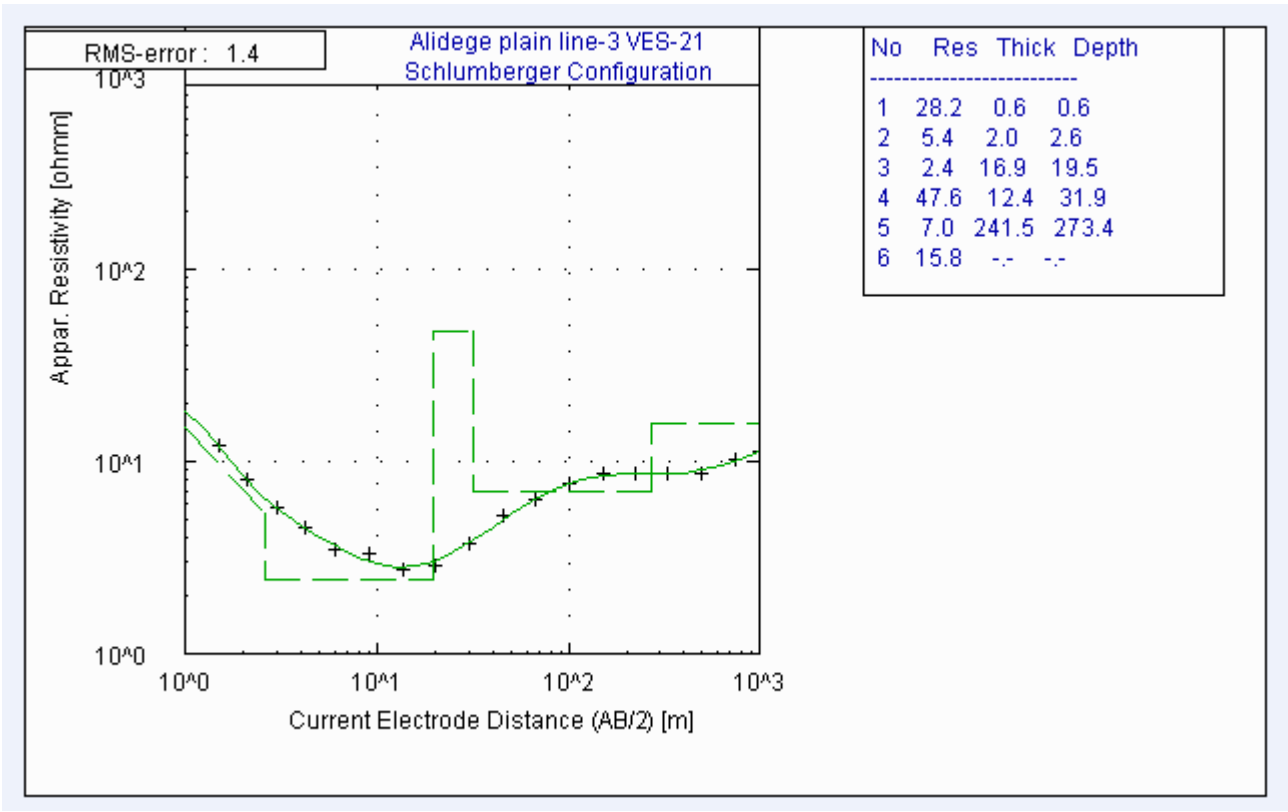
RMS-error : 1.4
Alidege plain line-3 VES-21
Schlumberger Configuration
Appar. Resistivity [ohmm]
10^3
10^2
10^1
10^0
10^0
10^1
10^2
10^3
Current Electrode Distance (AB/2) [m]
No Res Thick Depth
1 28.2 0.6 0.6
2 5.4 2.0 2.6
3 2.4 16.9 19.5
4 47.6 12.4 31.9
5 7.0 241.5 273.4
6 15.8 -.- -.-

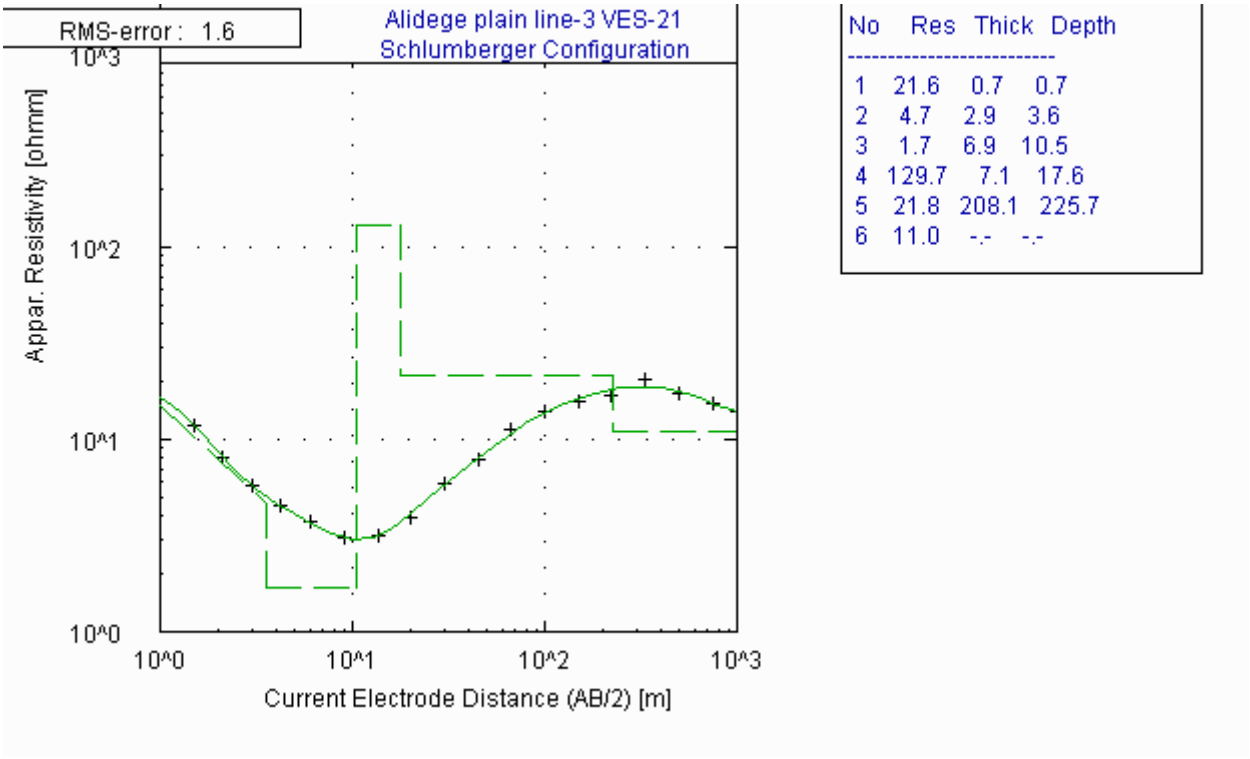
RMS-error : 1.6
Alidege plain line-3 VES-21
Schlumberger Configuration
Appar. Resistivity [ohmm]
10^3
10^2
10^1
10^0
10^0
10^1
10^2
10^3
Current Electrode Distance (AB/2) [m]
No Res Thick Depth
1 21.6 0.7 0.7
2 4.7 2.9 3.6
3 1.7 6.9 10.5
4 129.7 7.1 17.6
5 21.8 208.1 225.7
6 11.0 -.- -.-

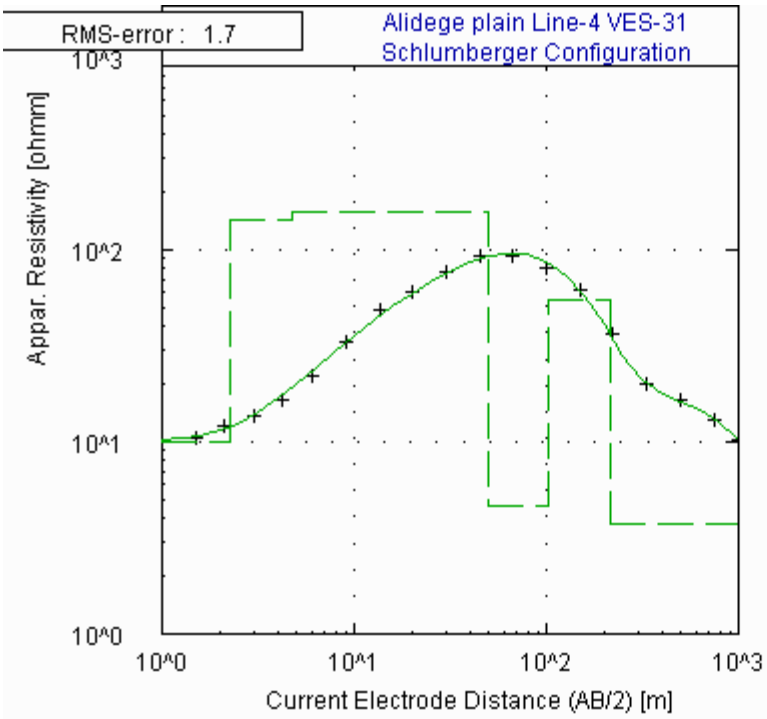

No	Res	Thick	Depth
1	10.1	2.2	2.2
2	144.6	2.5	4.7
3	159.5	45.3	50.0
4	4.7	52.5	102.5
5	55.0	111.0	213.5
6	3.8	-.-	-.-

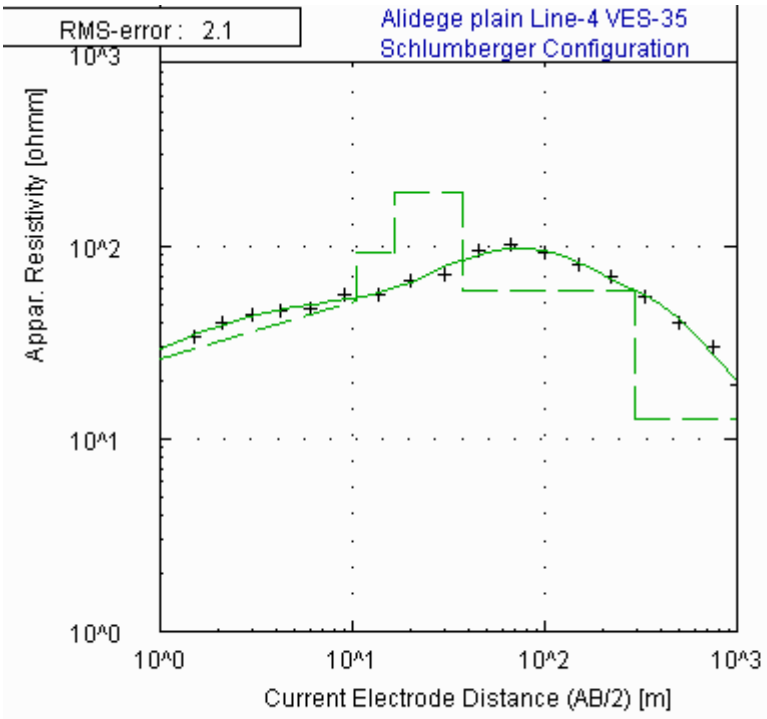

No	Res	Thick	Depth
1	21.2	0.5	0.5
2	52.8	10.1	10.6
3	93.4	5.8	16.4
4	190.6	21.4	37.8
5	59.0	256.4	294.2
6	12.8	-.-	-.-

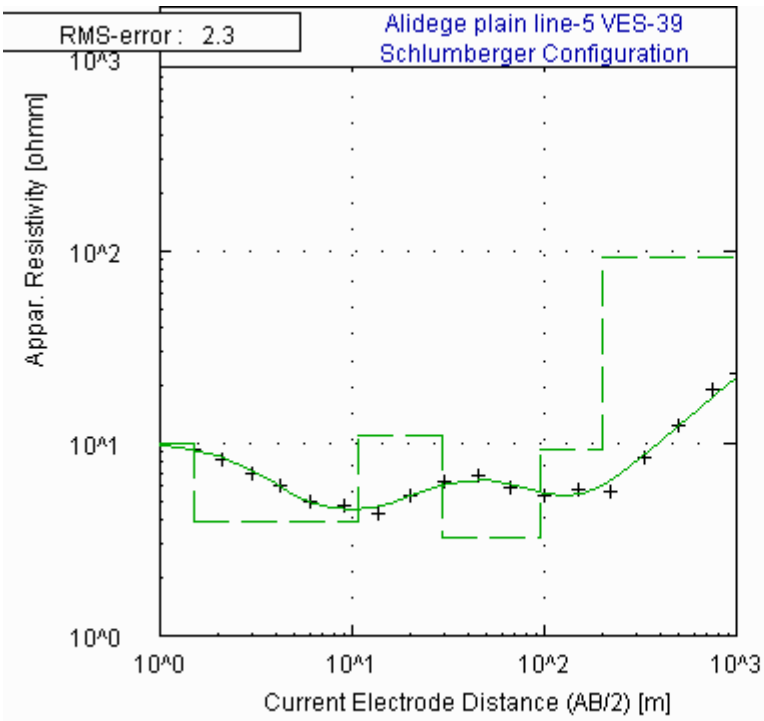

No	Res	Thick	Depth
1	9.9	1.5	1.5
2	3.9	9.3	10.8
3	10.9	18.6	29.5
4	3.2	66.2	95.7
5	9.3	102.5	198.1
6	92.3	-.-	-.-

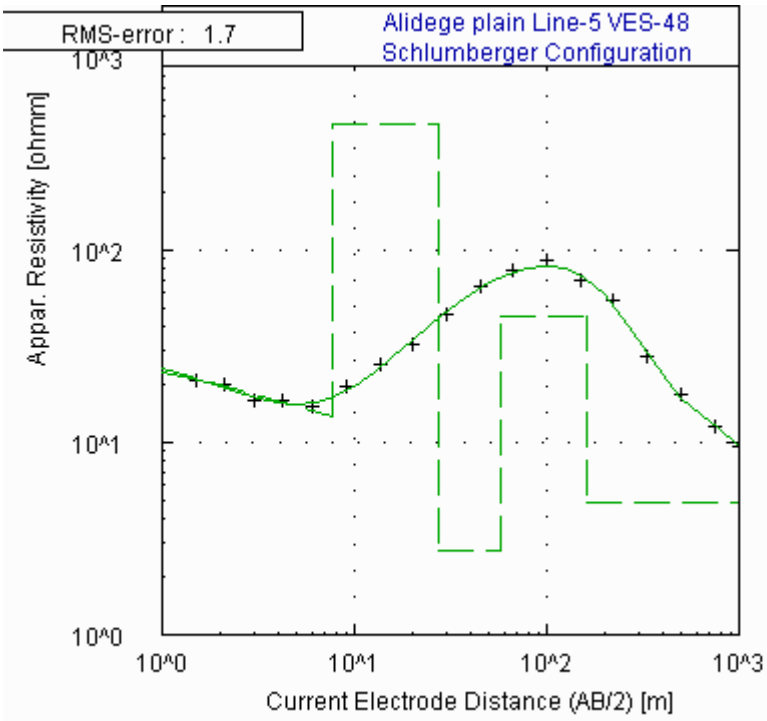

No	Res	Thick	Depth
1	24.2	1.0	1.0
2	13.6	6.7	7.6
3	454.8	19.8	27.4
4	2.7	30.7	58.1
5	45.2	102.8	160.9
6	4.9	-.-	-.-

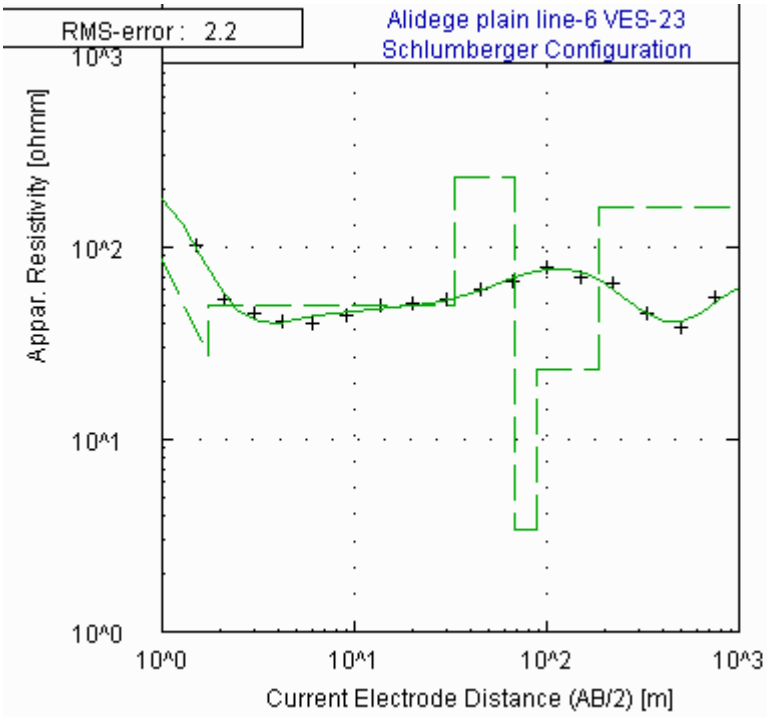

No	Res	Thick	Depth
1	309.2	0.6	0.6
2	27.6	1.2	1.7
3	49.8	31.1	32.9
4	233.9	35.5	68.4
5	3.4	20.1	88.5
6	22.9	96.1	184.6
7	160.6	-.-	-.-

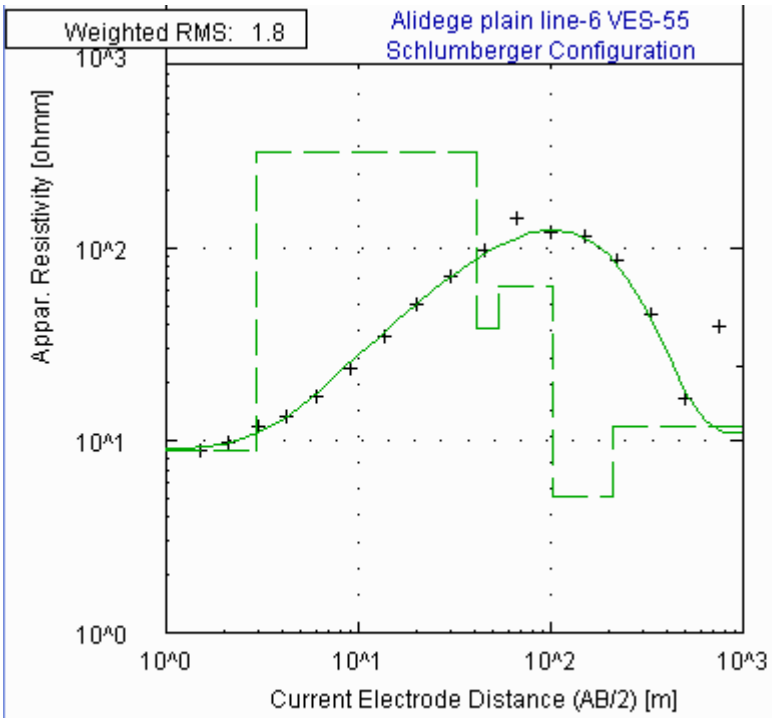

No	Res	Thick	Depth
1	9.0	3.0	3.0
2	319.0	38.1	41.1
3	38.4	12.8	53.9
4	63.7	49.4	103.3
5	5.1	109.5	212.8
6	11.8	-.-	-.-

ANNEX -2

Table 4.2 Lithological description of Borehole-12.

Depth	Description
0-6m	Clay
6-20m	Highly weathered & fractured Ignimbrite
20-22m	Highly weathered & fractured Basalt
22-36m	Highly weathered & fractured Ignimbrite
36-46m	Highly weathered & fractured Basalt
46-52m	Highly weathered & fractured Scoraceous Basalt
52-86m	Moderately fractured Basalt
86-92m	Highly weathered & fractured Scoraceous Basalt
92-102	Highly weathered Ignimbrite
102-114m	Moderately fractured Basalt
114-118m	Highly weathered & fractured Scoraceous Basalt
118-134m	Highly fractured Ignimbrite
134-152m	Moderately Fractured Basalt
152-160m	Moderately fractured Scoraceous Basalt
160-192m	Slightly Fractured Basalt
192-196m	Slightly fractured Scoraceous Basalt
196-208m	Slightly fractured Basalt
208-224m	Slightly fractured Scoraceous Basalt
224-230m	Slightly Fractured Basalt
230-238m	Slightly fractured Scoraceous Basalt
238-244m	Slightly fractured Basalt
244-252	Slightly fractured Scoraceous Basalt
252-266	Highly fractured Basalt
266-270	Slightly fractured Scoraceous Basalt
270-282	Highly Fractured Basalt
282-286	Highly fractured Basalt
286-294	Highly fractured Basalt
294-300	Highly fractured Basalt
300-310	Massive Basalt

Table 4.3 Lithological description of Borehole-2.

Depth	Description
0-4m	Ignimbrite
4-8m	Sand
8-12m	Moderately Weathered and fractured welded tuff
12-14m	Slightly weathered and fractured welded tuff
14-20m	Moderately weathered and fractured scoraceous Basalt
20-26m	Moderately weathered and fractured welded tuff
26-36m	Highly fractured and weathered vesicular Basalt
36-60m	Moderately fractured Basalt
60-80m	Highly fractured Basalt
80-100m	Moderately fractured Basalt
100-112m	Highly fractured scoraceous Basalt
112-130m	Slightly fractured scoraceous Basalt
130m-180m	Moderately fractured Basalt
180m-194m	Slightly fractured Basalt
194-200	Slightly fractured scoraceous Basalt
200-202m	Highly fractured Basalt
202-206m	Highly fractured scoraceous Basalt
206-218m	Tuff
218-242	Moderately fractured vesicular Basalt
242-252m	Welded Tuff

Table 4.4 Lithological description of Borehole-9

Depth	Description
0-4m	Clay
4-12m	Moderately weathered & fractured Ignimbrite
12-82m	Circulation loss
82-94m	Slightly fractured Basalt
94-104m	Highly weathered & fractured Scoraceous Basalt
104-106m	Moderately weathered Ignimbrite
106-112m	Moderately weathered Scoraceous Basalt
112-114m	Moderately fractured Ignimbrite
114-120	Slightly Fractured Basalt
120-128m	Slightly fractured Scoraceous Basalt
128-130m	Moderately fractured Basalt
130-140m	Moderately fractured Ignimbrite
140-150m	Moderately Fractured Scoraceous Basalt
150-162m	Moderately fractured Ignimbrite
162-182m	Moderately fractured scoraceous basalt
182-196m	Slightly fractured scoraceous basalt
196-204m	Slightly fractured Ignimbrite
204-250m	Highly fractured Ignimbrite

Table 4.5 Lithological description of Borehole-4

Depth	Description
0-4	Clay
4-12	Highly weathered and fractured Basalt
12-24	Slightly fractured scoraceous Basalt
24-86	Moderately Fractured Basalt
86-92	Slightly fractured Basalt
92-130	Moderately fractured Basalt
130-134	Slightly fractured Basalt
134-148	Moderately fractured Basalt
148-158	Slightly fractured Basalt
158-166	Highly fractured Basalt
166-180	Slightly fractured Basalt
180-190	Highly fractured Basalt
190-196	Moderately fractured Basalt
196-200	Welded tuff
200-206	Moderately fractured Basalt
206-210	Welded tuff
210-232	Moderately fractured Basalt
232-240	Welded tuff
240-246	Slightly fractured scoraceous Basalt
246-250	Moderately fractured Basalt
250-257	Slightly fractured Basalt

Table 4.6 Lithological description of Borehole-3

Depth	Description
0-2m	Clay
2-16m	Highly weathered & Fractured basalt
16-32m	Slightly fractured basalt
32-40m	Highly fractured Basalt
40-50m	Moderately fractured Basalt
50-52m	Ignimbrite
52-62m	Moderately fractured Basalt
62-72m	Highly fractured Basalt
72-74m	Ignimbrite
74-88m	Moderately fractured Basalt
88-98m	Bluish un welded tuff
98-104m	Moderately fractured Basalt
104-122m	Grayish unwelded tuff
122-140m	Slightly fractured scoraceous Basalt
140-148m	Moderately fractured scoraceous Basalt
148-178m	Bluish welded tuff
178-192m	Highly fractured Basalt
192-214m	Bluish un welded tuff
214-248m	Bluish welded tuff
248-258m	Moderately fractured Basalt
258-266m	Slightly fractured Basalt
266-282	Unwelded Tuff
282-294	Welded Tuff
294-304	Moderately fractured basalt
304-310	Moderately fractured Scoraceous basalt
310-350	Moderately fractured basalt